Plasma arising during the interaction of laser radiation with solids

V. S. Vorob'ev

Institute of High Temperatures, Russian Academy of Sciences, Moscow
(Submitted 17 June 1993; resubmitted 28 September 1993)
Usp. Fiz. Nauk **163**, 51–83 (December 1993)

The physical phenomena which result in the appearance of plasma near the surface of a solid heated by laser radiation are described. They include: the dynamics of heating and vaporization of the solid surface as a whole; separate defects of the surface, and aerosol particles; the hydrodynamics of the expansion of the vaporized material into the gas surrounding the target; and, the kinetics of ionization in the vapors or in their mixture with the surrounding gas. Plasma formation is linked, first, to the necessity of having sufficiently high vapor density in the interaction zone or to heating of the target up to a definite temperature, which imposes definite requirements on the energy parameters of the laser pulse. It is also linked to the possibility of development of ionization in the vapors or their mixtures with the surrounding gas; this dictates a definite laser-pulse intensity. Starting from these requirements, the boundary of the plasma region is found in the energy-intensity plane. The moment at which plasma appears is determined as the point of intersection of this boundary by the laser pulse in the same plane. Different cases of plasma formation in diffusion and hydrodynamic regimes of vapor efflux, associated with heating and vaporization of the target as a whole and its microdefects or aerosol particles, are described on the basis of this approach for different materials, pressures, and composition of the gas surrounding the target, size of the focusing spot, and durations, shapes, and wavelengths of the laser pulses.

1. INTRODUCTION

After high-power lasers were developed the range of phenomena accompanying the interaction of the radiation from these lasers with diverse solid targets, flat surfaces, and aerosol particles was investigated intensively. Melting, vaporization, emission of charged particles from the surface, and so on were studied. In the course of these investigations an interesting threshold phenomenon was observed—the appearance of plasma near the surface of the body (particle) irradiated by the focused laser beam. In the English literature this plasma is referred to as "laser induced (assisted) plasma created above a surface." In Russian literature the term "surface laser plasma (SLP)," underscoring the fact that the plasma arises near a surface, is usually employed.

In the experiments of Refs. 1–7, which were performed with ~ 1 μsec CO_2-laser pulses, it was observed that the laser radiation intensity required in order to produce plasma at solid surfaces is two-three orders of magnitude lower than the intensity required for plasma formation in a gas in the absence of solid surfaces. In atmospheric air plasma appears at metal surfaces with intensities $q \sim 10^7$ W/cm^2. In the absence of a surface breakdown of air under the same conditions occurs with $q \sim 10^9$–10^{10} W/cm^2. For millisecond and longer laser pulses q was found to be even lower: $\sim 10^5$–10^6 W/cm^2. A similar reduction of threshold for optical breakdown of gas by laser radiation was observed when suspended dust-like aerosol particles were present in the gas. Thus when air containing aerosol particles is irradiated with CO_2 or Nd laser pulses with duration of 200 and 50 nsec, respectively, this reduction reaches several orders of magnitude[8–10] and depends on the particle size, the radius of the laser spot, the wavelength of the radiation, and other factors.

The plasma radically alters the character of the interaction of radiation with matter. On the one hand the plasma itself partially or completely absorbs the laser radiation and thereby changes the fraction of the radiation reaching the surface; on the other hand, the plasma transfers energy to the body and seemingly plays the role of a nonlinear energy converter.

From the standpoint of laser technology the formation of plasma at the surface of the processed body can have both positive and negative effects. The plasma accelerates some chemical reactions at the surface, such as nitriding and boronizing.[11–12] At the same time, the appearance of plasma during precision operations, such as laser drilling, makes them much more difficult to perform.[13] The plasma of the vapors of the target material propagates with high velocity away from the surface and creates a reactive thrust. This idea is the basis for a design of a laser propulsion system,[14,15] which remains of interest to this day.[16]

Optical breakdown during the propagation of laser radiation in dispersed aerosol media is of interest in connection with the development of various systems—optical radar, remote sensing of the atmosphere, etc.

Thus it is obvious that it is necessary to determine the conditions under which an SLP arises for a given type of laser, shape and duration of the laser pulse, size of the focusing spot, material and state of the irradiated surface or aerosol particle, and type and pressure of the surrounding gas. These questions were partially touched upon in reviews and monographs.[17–28] In particular, in Ref. 25 the

 1063-7869/93/121129-29$10.00

history of research on the interaction of laser radiation with matter accompanied by plasma formation is described, and the pioneering works in this direction are indicated. In these works, however, the entire set of phenomena associated with SLP formation is described: dynamics of development of the plasma flame and propagation of the flame in space; dynamics of crater formation on the target surface and ejection of matter; measurements of the recoil pulse; screening of the laser radiation by the plasma; and, formation of photodetonation, ionization, and other types of waves and other phenomena. Very modest space was devoted to the original cause of the plasma formation. The authors confined their attention to describing different cases of SLP formation, focusing on various aspects of this phenomenon. Thus in one of the latest reviews on SLP (Ref. 28) attention was devoted mainly to the study of nonstationary gas-dynamic and optical processes occurring in a laser plasma after the first plasma focus has appeared. Inadequate attention is given to the plasma focus, though it is the plasma focus that determines the further evolution of the process. However, the threshold conditions under which SLP arises were investigated very intensively. Both early and later results which reveal the physical crux of this phenomenon have been obtained but are not reflected in the review literature. Information about SLP as a physical object and the reasons for the appearance of this object is very incomplete and dispersed over many papers. The theoretical models employed for interpreting the experimental results are very dissimilar and it is often very difficult to see any connection between them.

In the present review an attempt is made to generalize and systematize diverse cases of appearance of SLP and to put into some order our ideas about this physical object. The exposition is based on the fact that the initial formation of SLP is connected, as a rule, with the necessity of satisfying two quite general conditions (this is pointed out in Ref. 26). The realization of these conditions depends, first, on the initial focus of plasma initiation, associated with the state of the surface and the duration of the laser pulse, and, second, on the conditions of vapor efflux, which depends on the pressure of the surrounding gas and the temperature of the surface.

The review deals mainly with the interaction of laser radiation with solids with formation of low-temperature plasma. The intensity of the laser radiation falls in the range 10^5–10^{10} W/cm^2. This is the characteristic range for different regimes of technological processing of materials with cw, pulsed, and periodic-pulse lasers.[13,17,18,29] The pulse durations range from several nanoseconds to tens of milliseconds, the sizes of the focusing spots range from fractions of a millimeter to several centimeters. The typical parameters of the plasma are: electron density-10^{15}–10^{21} cm^{-3} and temperature-0.3–10 eV. The action of CO_2 or Nd lasers on different metals or dielectrics in different atmospheres is primarily considered.

Investigations of high-temperature thermonuclear laser plasma form a separate subject, to which a number of reviews and books are devoted.[30–34]

From the first experiments in which SLP were observed it became clear that the significant reduction in the intensity required for the formation of SLP is due to appearance of vapors of the target material in the laser-target interaction zone. First, the ionization potential of the vapors can be lower than that of the surrounding gas; second, when the vapor density is high enough, the vapor starts to absorb the laser radiation intensively, and this results in heating of both the vapors and their environment. These factors encourage development of ionization at the surface of the irradiated body. In order for a sufficient quantity of vapor to appear the laser radiation must heat to a sufficiently high temperature T the surface of the body or separate microscopic irregularities of the body or simply solid aerosol particles. This question as well as the dynamics of vapor efflux into the atmosphere has been investigated in many works (see, for example, Refs. 13, 15, 17, 18, 35–40). It is important to note that the rate of vaporization of a solid depends exponentially on the ratio Λ/T, where Λ is the specific (per unit mass) heat of vaporization of the target material. As a rule, this ratio is large. For this reason, at the first stage of heating the energy of the laser radiation absorbed by the body is removed by heat conduction or other heat-removal processes. Energy losses to vaporization are not significant. This happens until the temperature reaches some value T^*, after which the situation changes radically. Virtually all of the energy of the laser radiation goes into vaporization, and losses to heat conduction become insignificant. The temperature T^* is called the temperature of developed vaporization and the corresponding regime is the regime of developed vaporization (RDV).[2,3,15,18,19]

The second characteristic temperature T_b is the boiling or sublimation point of the target material under fixed pressure of the surrounding gas. This temperature separates regimes of vapor efflux. At temperatures $T < T_b$ the vapor pressure is much lower than the external pressure. The evaporating vapors diffuse into the surrounding gas, and a vapor-gas mixture (VGM) forms. This vaporization regime is called the diffusion regime (DR). For $T > T_b$ the vapor pressure is higher than the external pressure, and the evaporating vapors displace the gas surrounding the target. In the case of a flat target an erosion flame (EF) forms. This efflux regime is called the hydrodynamic regime (HR).

The temperature up to which the target must be heated is not known in advance. As we shall see below, it can be both less and greater (admittedly, insignificantly) than T^*. This is also true of the ratio of T^* and T_b. It should be noted that definite values of the laser energy density E (thermally insulated particle) at the target surface or approximately $E/t^{1/2}$ (surfaces), where t is the interaction time, are required in order to heat the target up to $T < T^*$. This is the thermal condition (TC). The thermal condition is the first necessary requirement in order to form SLP. However, it alone is not enough. A second, no less important, condition must be satisfied, and it is from this condition that the required temperature is found. We are talking about the possibility of developing ionization in the cloud of vapors or their mixture with the surrounding gas (the

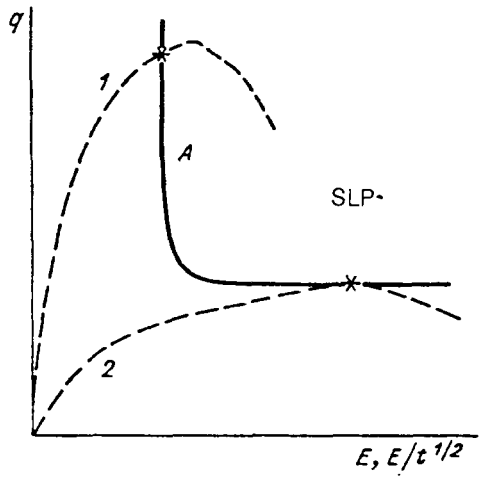

FIG. 1. Abscissa: E for thermally insulated targets and $E/t^{1/2}$ for surfaces; A is the breakdown line, SLP is the region of existence of plasma; *1*, *2*—laser pulses; the asterisks mark the moments at which plasma appears.

latter depends on the laser-target interaction conditions) which form during the interaction time—the ionization condition (IC). The ionization rate is proportional to the vapor density and, which is especially important, it depends exponentially on the temperature. If the vapor is in equilibrium, then this temperature is the temperature of heavy particles. In the nonequilibrium case it is the temperature of the electrons. It is important that the temperature depends on the absorbed laser energy and is a function of the intensity q of the laser radiation. For a definite value of q the ionization rate exceeds the rate of loss of electrons. The process is of a threshold character, since the ionization rate is an exponential function of the temperature and the intensity. Thus, for a known value of q we find from the IC the surface temperature and then from the TC the value of E or $E/t^{1/2}$. We obtain the relation between the breakdown values of q and E—the breakdown curve A, which determines the breakdown region in the E–q plane (Fig. 1). It is noteworthy that the laser pulse can be constructed in the same coordinates using the relation

$$E=\int_0^t q(t)\mathrm{d}t. \tag{1}$$

With the help of Eq. (1) it is easy to construct $q(E)$ from the known function $q(t)$. Figure 1 displays schematically a pulse 1 which intersects the breakdown curve A. The point of intersection (marked in Fig. 1 by the asterisk) where the laser pulse intersects the breakdown curve determines the breakdown values of E and q. Figure 1 also shows another pulse *2* which is tangent to the breakdown region. The point of tangency determines the threshold values of E and q for which a SLP first appears.

The approach based on this qualitative picture makes it possible to describe in the same manner many cases of formation of SLP for laser pulses with different wavelength, shape, and duration and for different sizes and volume of the focal region, for targets made of different materials and surrounded by different gases. The problem consists of finding the threshold values of E and q which depend on the specific form of the TC and the IC.

The form of the TC depends mainly on the state of the surface and the shape and duration of the laser pulse. The surface of the body, as a rule, is not perfectly smooth, but rather it contains different microscopic irregularities, foreign inclusions, and so on. The laser radiation heats the surface nonuniformly and the heating depends significantly on the duration and intensity of the laser pulse. For laser pulses with duration $\tau > 10^{-4}$ sec and intensity 1–10 MW/cm^2, as a rule, there is enough time for the temperature of the surface to equalize during the heating process and it is possible to talk about heating of the surface as a whole. It is useful to combine all such cases of SLP formation into a separate group—S. As the leading edge of the laser pulse becomes shorter, the duration of the pulse becomes shorter, and the intensity of the pulse increases somewhat, different types of microscopic irregularities and defects, which are always present on the surface, become more important for plasma formation. Thus for laser pulses with $\tau < 10^{-5}$ sec and intensities 10–500 MW/cm^2 plasma formation is associated entirely with heating and vaporization of such microscopic defects in the surface. Thermally insulated microscopic defects are heated first.[19,40–43] We also combine into a separate group (MD) the cases when SLP forms due to heating and vaporization of microscopic defects.

We place into a third group A surface laser plasma initiated by heating and vaporization of aerosol particles. This group is in many ways similar to the microdefect group, though, of course, plasmas in group A have their own peculiarities, associated, primarily, with the specific nature of the absorption of laser radiation.[44–46] The TC for each of these groups will reflect the specific nature of the heating.

The ionization condition largely depends on the regime of efflux of vapor. In the diffusion regime in a VGM ionization develops in the mixture of the vapors and the surrounding gas. As a rule, the laser radiation heats the electronic component of this mixture. The electrons transfer energy to the heavy component. If the heavy component is an atomic gas, energy transfer is impeded and the temperature of the electrons can become decoupled from the temperature of the heavy particles. When the heavy component is a molecular gas, however, energy is exchanged rapidly and the mixture is heated with a single temperature. Electrons are produced due to ionization of the vapor atoms in collisions with electrons and are removed as a result of diffusion into the cold regions.

Development of ionization in an erosion flame in the hydrodynamic regime occurs in the pure vapors of the target material. Here convective removal of electrons, owing to directed motion of the vapor jet, can become the main form of electron loss.

The different cases of formation of SLP are summarized in Table I. The cells of this table with the "+" sign correspond to the states studied in the present review. Thus, S–VGM–m means that the SLP is formed as a result of heating of the surface as a whole in the diffusion regime

TABLE I.

IC \ TC		S	MD	A
VGM	a	+		+
	m	+		+
EF		+	+	+

of vapor efflux into a molecular gas surrounding the target; A–EF means that the SLP forms due to heating and vaporization of aerosol particles in the hydrodynamic regime of vapor efflux; and so on.

The proposed classification determines, to a significant degree, the structure and content of this review. In Sec. 2 we consider the characteristic features of the interaction of laser radiation with a smooth surface, microscopic defects on the surface, and aerosol particles and the specific nature of the development of ionization in vapor-gas mixtures and in erosion flames. In subsequent sections the specific states of SLP in accordance with the proposed classification are described. The TC and IC, from which the threshold values of E and q are determined, are given and the values are compared to the experimental data. The physical features of one or another state of a SLP are discussed.

2. CHARACTERISTICS OF THE INTERACTION OF LASER RADIATION WITH SOLIDS

2.1. Characteristics of heating of the surface

The possibility of absorption of laser radiation depends significantly on the state of the irradiated surface—the degree to which the surface is contaminated by foreign impurities, the existence of an oxide film and microscopic irregularities, and the presence of physically or chemically adsorbed substances. In contrast to the parameters of the radiation and the properties of the gas surrounding the target, it is extremely difficult to describe completely the state of the surface. It is no less difficult to monitor the state of the surface during the experiment. Nonetheless, in the last few years a number of factors which characterize the the state or the surface and strongly influence the absorption of laser radiation have been studied. We now briefly discuss these factors.

The first factor is associated with the nonuniformity of the surface material itself and the presence of different chemical compounds, having different absorption coefficients, on the surface. Thus samples of aluminum alloys AL-9, AL-24, and AL-23, which had been subjected to mechanical polishing with an abrasive and diamond grinding, were investigated in Ref. 47. The microstructure of the AL-9 samples contains inclusions of a second phase Mg_2Si and $CuAl_2$.[48] The AL-23 samples also have particles of a second phase with the composition Al_3Mg_2, Al_2Ti, and Al_3Zr which are embedded in the matrix. These particles differ from particles of the AL-9 samples in that they are larger and their surface density distribution is lower. The even lower density and larger sizes of particles of the second phase (up to 100 μm), consisting of $MnZn_2$ and $Al_2Mn_3Zn_3$, are obtained on the surface of AL-24 samples. The sizes, composition, and distribution density of the particles of the second phase over the surface determine the optical absorption of the incident radiation, which becomes nonuniform due to the difference in the reflectances at the wavelength $\lambda = 10.6$ μm. Investigations showed that the higher the surface density distribution of the particles of the second phase, the greater the absorption of laser radiation is and the lower the intensities at which plasma arises are.

Photographs of the surface of an aluminum sample, which were obtained in a scanning electron microscope, are displayed in Ref. 49. Lighter colored sections (aluminum oxides) can be seen in them. The typical sizes of these sections are 1-10 μm, and their surface density $n \sim 10^6$ cm^2. After the samples are irradiated with a series of pulses the sizes and concentration of nonuniformities of this type decreased. Adsorption, by the surface, of impurities from the surrounding medium or the volume of the material increases the surface absorption.

Together with such foreign inclusions, whose chemical composition is different from that of the main material, there also exist microscopic irregularities consisting of the material itself. These include flakes, irregularities, points, and microcracks. Due to the fact that most of the surface is partially or completely thermally insulated from the material, microscopic irregularities of this type can heat up more rapidly than the main surface. This is especially true for the flakes, whose thermal contact with the surface is insignificant. Photographs of these defects are presented in Ref. 49. The thicknesses d of these defects are fractions of a micron and their concentrations are 10^3–10^4 cm^{-2}. The surface density of irregularities and defects which are in thermal contact with the substrate is much lower density. Their size and shape depend on the method of surface treatment.[50]

Defects play an important role in the radiation strength of optical materials.[51,52] Finally, we note that even on an impurity-free surface local regions where the field is intensified[53] and which also lead to more intense vaporization of matter arise due to the presence of defects in the form of small channels, cracks, surface pits, and so on. A real surface contains many defects. For this reason, for a specific laser pulse, whose leading edge has a definite duration and rise time, there is always a group of defects that act as initial centers of vaporization.

The problem of laser heating of a surface containing different types of microscopic irregularities and defects is extremely difficult and virtually impossible to solve completely due to the lack of complete information about the state of the surface. The problem is usually divided into a series of simpler problems, which represent different limiting cases.

2.2. Perfectly smooth surface

The fraction of the laser radiation absorbed by a perfectly smooth surface, which does not contain foreign inclusions and impurities, can be written in the form $\zeta q(t)$,

TABLE II.

Target	Zn	Pb	In	Brass	Ti	Ni	Al	Cu	Nb	Ta	W	C	Al_2O_3	SiO_2
ζ, %	9	10	11	10	11	5	5	<5	8	8	<8	40	90	80

where ζ is a dimensionless absorption coefficient, which, generally speaking, depends on the surface temperature. Table II gives the absorption coefficients (taken from Ref. 23) averaged over the temperature interval from room temperature up to the boiling point. Obviously, metals do not have high absorption coefficients, while strongly absorbing materials such as C and Al_2O_3 have significantly higher absorption coefficients.

Let a laser beam with intensity $q(t)$, surface energy density $E(t)$, and focusing-spot size R be incident normally on the flat surface of a target. According to Refs. 17, 54, and 55, in the one-dimensional formulation of the problem the temperature, determined by solving the heat-conduction equation in the half-space with energy released at the boundary with no vaporization, at the center of the focusing spot under the condition that $4\chi t/R^2 \ll 1$ is determined by the expression

$$T(t)=[\zeta/c\rho(\sqrt{\pi\chi})^{1/2}]\int_0^t q(u)\mathrm{d}u/(t-u)^{1/2}, \qquad (2)$$

where $\varkappa=\chi\rho c$ is the thermal conductivity of the target material, χ is the thermal diffusivity, and ρ and c are, respectively, the density and heat capacity of the target material.

The equation (2) is valid until intense vaporization of the target material starts. The rate of vaporization can be written in the form

$$v=v_0(T_b/T)\exp(-\Lambda A/RT), \qquad (3)$$

where v_0 is of the order of the sound speed in the cold metal, A is the atomic weight of the target material, and R is the universal gas constant. As we can see, v depends extremely sharply on the temperature and, for this reason, at some moment, according to Eq. (2), the temperature stops increasing and the regime of developed vaporization, when the energy of the laser beam goes mainly into vaporizing particles of the condensed phase and partly imparting kinetic energy to them, is realized. In this case

$$\zeta q=\rho v[\Lambda+(bRT/A)]. \qquad (4)$$

In Eq. (4) b is a numerical factor that depends on the regime of vapor efflux. For efflux of a perfect gas of vapors into a gas with counterpressure $b=5/2$.[18] Due to the sharp dependence of v on T the transition from Eq. (2) to Eq. (4) will occur in a narrow range of values of E and q, so that there exists a temperature T^* (Ref. 13) such that Eqs. (2) and (4) hold simultaneously. It is convenient to write the relations (2) and (4) in dimensionless units. We introduce $E'=E/E_v$, $q'=q/q_v$, $T'=RT/\Lambda A$, $t'=tv_0^2/9\chi\pi$, where

$$E_v=9\rho\chi\Lambda/\zeta v_0 \qquad (5)$$

For Cu, for example, with $\zeta=0.05$ we obtain $E_v=4.8$ J/cm^2 and $q_v=4.8\cdot 10^{11}$ W/cm^2. In dimensionless units the relation (2) assumes the form (primes are dropped)

$$T=\int_0^t q(u)\mathrm{d}u/(t-u)^{1/2}, \qquad (6)$$

and the relation (4) is

$$q=(1+bT)\exp(-1/T). \qquad (7)$$

The equations (6)–(7) give a parametric relation (parameter T) between q and the quantity

$$L=\int_0^t q(u)\mathrm{d}u/(t-u)^{1/2}. \qquad (8)$$

It is important to note that both depend only on the shape of the laser pulse. It is easy to calculate L for pulses with a power-law intensity $q\sim t^\alpha$:

$$L=(E/t)^{1/2}f(\alpha),$$

where

$$f(\alpha)=(\alpha+1)\int_0^1 u^\alpha\mathrm{d}u/(1-u)^{1/2}$$
$$=\sqrt{\pi}(\alpha+1)\Gamma(\alpha+1)/\Gamma(\alpha+3/2).$$

is a numerical factor that depends on the exponent α. Table III gives values of $f(\alpha)$ for different values of α. In particular, for a pulse with constant intensity $\alpha=0$ and $E=qt$ we easily find from Eqs. (7)–(8) the time corresponding to onset of RDV[18]

$$t=T^2\exp(2/T)/(1+bT)^2.$$

The quantity L can also be calculated explicitly for a very short intense pulse, "switched on" at time t_1, such that the pulse can be approximated by a δ-function $q(t)=E\delta(t-t_1)$. In this case $L=E(t-t_1)^{1/2}$. We can see that for a wide class of functional dependences $q(t)$ we obtain $L\sim E(t)/t^{1/2}$. For a pulse whose shape is not described by these functions, L must be calculated using Eq. (8): this does not present any special problems for existing computers.

A universal family of lines of constant temperature (isotherms) can be constructed in the L–q plane with the help of Eqs. (6) and (7). Equation (6) will correspond to vertical sections of the isotherms and Eq. (7) will correspond to horizontal sections. The points of intersection

TABLE III.

α	−0,9	−2/3	−1/2	0	1	2	3	4
f	1,91	1,41	$\sqrt{\pi}/2$	2	8/3	16/5	128/35	256/63

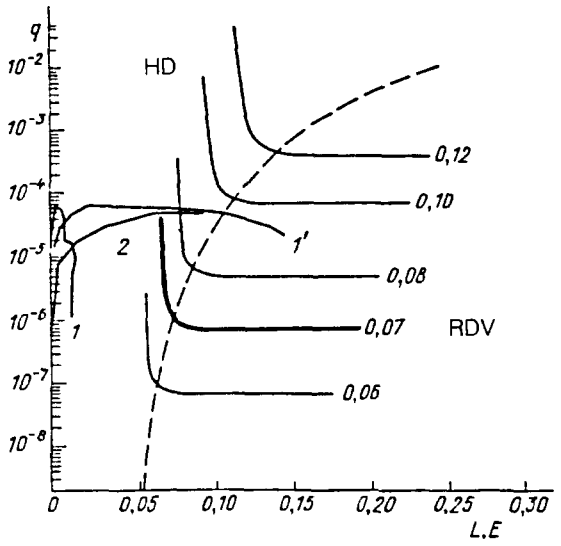

FIG. 2. Plane of the dimensionless variables q—L or E in which isotherms are plotted ($T=0.06$, 0.07, 0.08, and so on). The dashed curve separates this plane into regions in which the regime of developed vaporization (RDV) and the heat-conducting regime (HD) are valid. The isotherm $T=0.07$ (distinguished by the thick line) corresponds to the boiling point being reached for copper. The diffusion regime lies to the left of this isotherm; the hydrodynamic regime lies to the right. *1*, *1'*—pulses from Ref. 56, constructed for a surface and for microdefects, respectively; *2*—pulse from Ref. 23 for a surface.

form a curve—the curve of RDV—on which Eqs. (6)–(7) hold simultaneously. This curve separates the L–q plane into two regions. In the region above the curve heating is determined exclusively by heat conduction—the heat conduction regime (HR). The region below the curve will correspond to the RDV. This is shown in Fig. 2, where such a curve (1) is constructed and the isotherms are plotted.

The temperature T^* is not related to T_b and it is possible to have cases with $T^* > T_b$ and $T^* < T_b$, i.e., the RDV is possible in both the diffusion and hydrodynamic regimes. For metals the ratio T_b/Λ does not vary too strongly and lies in the range 0.05–0.09.[15,25] In addition, low-melting metals (Zn, Pb) and refractory metals (W, Ta) correspond to extreme values. In Fig. 2 the isotherm $T=0.07$, corresponding to heating of the metal up to the boiling point, is singled out. The region below or to the left of this isotherm corresponds to the diffusion regime of vapor efflux and the region above this isotherm corresponds to the hydrodynamic regime.

The laser pulse can be reconstructed in the same coordinates. Its position in the plane depends on the surface material. The point of intersection of the pulse with the curve gives the instantaneous values of L and q corresponding to the onset of the RDV. The pulse employed in Ref. 56 for a copper target $\zeta=0.05$ (curve *1*) is plotted in Fig. 2. This is a typical pulse for TEA lasers. Its total energy is 20 J/cm^2 and the pulse duration is 3500 nsec. The intensity at the peak at $t=80$ nsec reaches $2.8\cdot 10^7$ W/cm^2, after which the intensity drops off linearly from the maximum value to $0.86\cdot 10^7$ W/cm^2 at $t=270$ nsec and from this value to zero by the end of the pulse. As one can see, RDV is not reached in the case when a flat target is heated by this pulse. As we shall see below, however, this pulse is very effective for heating and vaporizing microdefects.

Another pulse, employed in Ref. 23 for copper (curve 2), is plotted in the same figure (Fig. 2). The duration is ~ 1 msec, the intensity is constant and equal to ~ 20 MW/cm^2, and the rise time is ~ 0.1 msec. Here the RDV is realized immediately following the hydrodynamic regime. This pulse is very effective for heating and vaporizing a flat target.

It is obvious that in a number of cases a definite value of $E(t^*)/t^{*1/2}$, characterizing the laser pulse, is required in order to heat a perfectly smooth surface up to $T=T^*$ in the absence of developed vaporization. For a given material this ratio depends only on its thermophysical characteristics. In Ref. 57 it is suggested that the onset time of plasma formation t^* be defined as the moment when $E^*/t^{*1/2}=10$ J/cm$^2\cdot\mu$sec$^{1/2}$, since the experimental data of Ref. 58 satisfy this empirical dependence. It is clear from what we have said above that this method for determining the moment of plasma formation is by no means universal, and much existing of experimental data do not conform to this dependence.

2.3. Thermally insulated microdefects

The breakdown concept based on heating of a surface up to the temperature of developed vaporization and subsequent development of ionization in the vapors formed is not valid in the case when a target with high radiation strength is exposed to microsecond pulses.[26] Thus breakdown of air at metallic mirrors under the action of a neodymium laser with a 0.4 μsec pulse focused into a 0.5 cm in diameter spot was investigated in Ref. 41. For Al the calculations give an increase in the surface temperature of only 20–200 °C. The recorded brightness temperature is significantly higher. A nonuniform "point" glow structure is characteristic for all mirrors investigated. The density of such points fluctuates strongly for different materials. Thus for an aluminum mirror it is $5\cdot 10^4$ cm^{-2}, while for steel and copper mirrors it is more than two orders of magnitude lower. The brightness structure is determined by the presence of microdefects.

A similar picture was observed in Ref. 42 under the action of a 1.5 μsec CO_2 laser pulse with a 0.2 μsec spike on an aluminum target. Points began to glow even before breakdown of the air at the target surface; microflames, merging into a single plasma flame, developed from these hot points. The density of hot points was $2\cdot 10^5$ cm^{-2}. The threshold energy density for breakdown in these experiments was ~ 1.7 J/cm^2, and for 10^{-7}–10^{-8} sec pulses it did not depend on the pulse duration.

Thin layers of metal (flakes) which are thermally insulated from the substrate are the most easily heated and vaporized surface defects. The thickness d of such defects is fractions of a micron, and the linear size $S^{1/2}$ (where S is the area) can reach tens of microns. The flake concentration n depends on the method of surface processing and fluctuates from 10^3 to 10^5 cm^{-2}.

The following characteristic dimensions are important in the case when a microdefect absorbs electromagnetic radiation: $\lambda=2\pi c/\omega$—the wavelength of the incident radiation with frequency ω in the external medium; $\delta=\lambda/|\varepsilon|^{1/2}$—the wavelength of the electromagnetic field in the defect material with permittivity ε; and, the characteristic dimensions of the defect itself. In the case $S^{1/2}\geqslant\lambda$ diffraction effects can be neglected and absorption by a flake can be described approximately as absorption by a thin film of thickness d separated from the matrix by a dielectric substrate of thickness $h\sim d$. For $d\leqslant\delta$ interference effects are important and the problem of the incidence of a monochromatic plane wave on such a system must be solved. The solution is presented in Ref. 60. The calculations performed in Ref. 61 showed that at thicknesses $d>0.08$ μm ζ for a flake is virtually independent of d and corresponds approximately to absorption by a continuous material.

In the case when a flake is heated from room temperature up to a temperature of the order of the temperature T^* of developed vaporization we shall not describe the melting process, since $\Lambda_m\gg\Lambda$, where Λ is the specific energy of melting, and the process is secondary. We assume that $d^2/\chi\gg t$, where t is the heating time of the flake up to a temperature of the order of T. In this case the flake is heated as a whole. The simplest equation for the change in temperature of the flake up to the onset of developed vaporization has the form

$$dc\rho\mathrm{d}T/\mathrm{d}t=\zeta q(t). \tag{9}$$

Integrating Eq. (9) for the temperature from zero to T we obtain

$$E=c\rho Td/\zeta. \tag{10}$$

If the heating times are such that there is not enough time for the flake to be heated as a whole but rather only a layer of the flake of thickness of the order of $(\chi t)^{1/2}\ll d$ is heated, then we obtain instead of Eqs. (9)–(10)

$$T=\zeta E/(\chi t)^{1/2}c\rho\approx\zeta q(\chi t)^{1/2}/\varkappa,$$

This equation is identical, to within a numerical factor, to Eq. (2) for the heating of a perfectly smooth surface. In this case the thermally insulated flake and surface are heated almost identically and the microdefect plays no role in plasma formation.

For a flake we can introduce, just as for a smooth surface, the temperature T^* of developed vaporization such that for $T\geqslant T^*$ all laser energy goes mainly into vaporization. At the temperature $T=T^*$ Eq. (5) must hold together with Eq. (10). Introducing dimensionless variables for q and T, just as in the case of a surface, and for E, in accordance with Eq. (10) ($E'=E/E_v$, where $E_v=c\rho A\Lambda d/\zeta R=3\rho\Lambda d/\zeta$), we obtain an equation for developed vaporization for a flake:

$$E^*=T^*,\quad q^*=(1+bT^*)\exp(-1/T^*). \tag{11}$$

The difference of Eq. (11) from Eqs. (7)–(8) is associated with the fact that the heating equation is different for a flake. The plot in Fig. 2 can likewise be employed in order to determine the region of RDV, plotting E instead of L along the abscissa. We reconstruct in these coordinates the pulse from Ref. 56, used above, assuming that the pulse acts on a copper target whose surface contains flakes with thickness $d\sim0.2$ μm. Now it assumes the form 1′. Here the RDV is achieved, and such a pulse can completely vaporize a microdefect and lead to the formation of SLP, as observed in Ref. 56.

We now write the simplest equation for the dynamics of vaporization of a flake in the region of RDV:

$$\Lambda\rho\mathrm{d}d/\mathrm{d}t=\zeta' q(t), \tag{12}$$

where ζ' is the average absorption coefficient for laser radiation in the temperature range $T>T^*$. According to numerous experimental data,[15] after the onset of intense vaporization of the material the absorptivity of the material increases appreciably. Integrating Eq. (12) from t^* up to the moment of complete vaporization of the flake we find the time dependence of the thickness of the flake

$$d(t)=d-(\zeta'/\rho\Lambda)(E(t)-E^*). \tag{13}$$

Hence the energy density required for complete vaporization of the defect is

$$E_t=E^*+d\rho\Lambda/\zeta=E^*[1+(\Lambda\zeta'/cT^*\zeta)]. \tag{14}$$

For $T>T^*>T_b$ vapors displace the surrounding gas. It is of interest to estimate the size of the vapor cloud. A detailed hydrodynamic calculation of the expansion of the vapor with varying conditions at the boundary is possible only by numerical methods. In our case, however, not all details of the flow are equally important. It is important to describe correctly the region where the main mass of vapor is concentrated. For this we consider the well-studied qualitative picture of hemispherical expansion of vapor.[17] The boundary of the Knudsen layer, on which the hydrodynamic flow velocity is equal to the local velocity of sound, is located near the surface of the body. This is followed by a region of supersonic flow, separated from the following region with subsonic flow by a stationary shock wave, a so-called "suspended shock." For spherical particles with radius r the size of the region of supersonic flow is given by the expression $R_s=0.59r(p_0/p_\infty)^{1/2}$, where p_0 is the pressure on the body and p_∞ is the pressure of the surrounding gas. For laser radiation intensity $q\sim1$–60 MW/cm^2 we have $R_s\sim(1$–$3)r$. It is much more difficult to determine the size of the region of supersonic flow for nonspherical particles than for spherical particles. It is important to note, however, that the main mass of the vapor is concentrated in the region of sonic flow between the stationary shock wave and the contact boundary between the vapor and the surrounding gas. For the spherically symmetric case the distance to the contact boundary is $R\gg R_s$. It is this distance that determines the instantaneous size of the vapor cloud. The velocity of the contact boundary is low compared to the velocity of sound, and the vapor temperature near the contact boundary is close to the boiling point. The vapor density in the subsonic region is virtually constant and equals[17]

$$\rho_v = mp_\infty / 0.67kT_b \quad (15)$$

where m is the mass of a vapor atom and γ is the ratio of specific heats. Neglecting the deviation of the vapor density from Eq. (15) in a small region of the supersonic flow, we find from the law of conservation of mass of the vapor for a flake an expression for the size of the vapor cloud as a function of time during the process of vaporization of the microdefect:

$$R(t) = [(3\rho/2\pi\rho_v)(d - d(t))]^{1/3}$$
$$= [(3\zeta'/2\pi\rho_v\Lambda)(E - E^*)S]^{1/3}. \quad (16)$$

The radius of the vapor cloud reaches its maximum value when the flake is completely vaporized:

$$R_m = (3\rho dS/2\pi\rho_v)^{1/3}. \quad (17)$$

2.4. Roughness

In Refs. 57 and 58 heating of surface irregularities by the laser radiation is studied together with a smooth surface and flakes. The absorption coefficient ζ' of the irregularities can differ from the absorption coefficient of a smooth surface. For hemispherical protuberances with radius a the absorption cross section in the case $\lambda \gg a$ but $\delta \ll a$ has the form[60]

$$\sigma = 3\pi a^2 \zeta,$$

which is three times greater than the area of the base multiplied by the absorption coefficient. In the case $\lambda \ll a$ and $\delta \ll a$, however, absorption becomes similar to absorption by a section of flat surface with area πa^2, i.e., $\sigma = \pi a^2 \zeta$.

It is assumed that a protuberance is heated rapidly up to some temperature, but, in contrast to a flake, it exchanges heat with the substrate. The equation describing the heating of the irregularity has the form

$$\rho c V \mathrm{d}T/\mathrm{d}t + \alpha S T = \zeta' q(t), \quad (18)$$

where V and S are the volume and base area, respectively, of the protuberance and α is the coefficient of heat transfer into the mass of the material. We write the solution of Eq. (8) in the form

$$T(t) = [S\zeta' \exp(-\alpha St/\rho cV)/\rho cV]$$
$$\times \int_0^{\pm} \mathrm{d}t' q(t') \exp(-\alpha St'/\rho cV). \quad (19)$$

The exponent in the exponential in Eq. (19) characterizes the heat exchange between the protuberance and the substrate. In order of magnitude $\alpha St/\rho cV \sim \chi t/d^2 \sim t/t_d$. If $t/t_d \ll 1$, the solution (19) passes into Eq. (10)—the case of total thermal insulation. The inverse case $t/t_d > 1$ is more interesting. Then we write the solution (19) approximately as

$$T(t) \approx \zeta q(t)/\alpha \approx q(t) d\zeta'/\chi\rho c.$$

Hence it is easily found that for heating of an irregularity up to T requires

$$E \sim Et\zeta/2t_d\zeta'. \quad (20)$$

2.5. Aerosols

The presence of suspended dust-like particles in the gas results in additional absorption of laser radiation, heating and vaporization of these particles, ionization of the vapors formed, and formation of plasma. In spite of the fact that there is much in common between plasma formation on the boundary of condensed media (macrotargets) and in a gas with aerosol particles, there are also significant differences. Here we consider the fundamental points, and we refer the reader to the literature devoted to the interaction of laser radiation with aerosols for the details.[8–10,42–48,62–69]

The first distinction is associated with the nonuniformity of the optical field inside an aerosol particle. As a rule, there arises a principal maximum (PM) of the optical field, the position of the maximum being determined by the center of intense heat release in the particle. In weakly absorbing particles the PM forms in the shadow hemisphere.[62] The nonuniformity of the field over the particle can lead to fragmentation of the particle and formation of smaller particles. This occurs, for example, in the case when quartz particles with size $r = 20$–80 μm are irradiated with TEA-CO_2-laser radiation with energy density of several J/cm^2.[63] The fragment sizes fall in the range $r = 0.5$–3 μm. In relatively small particles the field becomes approximately more uniform.[64] This is equally true for the temperature, which, due to heat conduction, can be equalized even with a nonuniform field. We confine our attention below to such cases and consider the model of absorption of laser radiation by an aerosol particle following the results of Refs. 19, 65, and 68.

Absorption of electromagnetic radiation by a spherical particle depends on the complex index of refraction $n = n' + i\varkappa$, the wavelength of the radiation, and the particle material and size. The values of n' and $\varkappa$ at different wavelengths are presented in Ref. 70. The absorption coefficient is given by the well-known formula

$$K = 4\pi\varkappa/\lambda. \quad (21)$$

The absorption cross section for $Kr \gg 1$ is determined by the expression

$$\sigma = \pi r^2 \zeta. \quad (22)$$

For strongly absorbing materials, such as carbon, the average value is $\zeta \sim 1$ at temperatures $T \leqslant T_b$. For the case of weak absorption ($Kr \ll 1$) and assuming the diffraction equation $2\pi r/\lambda \ll 1$ is satisfied, Rayleigh's formula[71] can be used for the absorption cross section:

$$\sigma = \pi r^2 (2\pi r/\lambda); \quad (23)$$

$h_\lambda = 24n\varkappa/[(n^2 - \varkappa^2 + 2)^2 + 4n^2\varkappa^2]$. The calculations performed in Ref. 68 using the data of Ref. 70 give, for example, for soot $h_\lambda = 0.96$ ($\lambda = 10.6$ μm). For comparison we note that $h_\lambda = 0.26$ for polycrystalline graphite and 0.045 for single-crystalline graphite. It is evident that absorption strongly depends on the state of the absorbing material. Usually a critical radius r_c is introduced. It is defined so that for $r = r_c$ Eqs. (17) and (18) are identical. This gives

$$r_c = \lambda\zeta/2\pi h_\lambda. \quad (24)$$

For carbon irradiated with CO_2-laser radiation the quantity ζ and h_λ are close to 1, so that r_c is virtually identical to the wave number, as in the case of absorption in metals.[71] We write finally

$$\sigma=\pi r^2\zeta z(r), \tag{25}$$

where $z(r)=1$ if $r\geqslant r_c$ and $z(r)=r/r_c$ if $r<r_c$.

Heating of a spherical particle by laser radiation has been studied in many works (see, for example, Refs. 44–46 and 72), where laser heating and vaporization processes were studied taking into account phase transformations, heat and mass exchange with the surrounding medium, and the temperature dependences of the optical and thermophysical characteristics of the particle material and the gas-dynamic parameters of the vapor-gas medium. However, under conditions such that $\chi t^*/r^2\gg 1$, where t^* is the time when $T=T^*$, the particle is heated as a whole and we can write

$$(4\pi r^3/3)c\rho dT/dt=\zeta\pi r^2 q(t)z(r). \tag{26}$$

Integrating Eq. (21) we obtain

$$E^*=4c\rho T^* r/3\zeta z(r). \tag{27}$$

As one can see from Eq. (27), for $r\gg r_c$ we have $E^*\sim r$, and for $r\ll r_c$, correspondingly, $E^*\sim r_c$. The equation (27) is essentially the same as Eq. (10) for heating of a thermally insulated defect. For this reason, the limits of the RDV can be determined with the help of the plot in Fig. 2, scaling E in accordance with Eq. (27).

For $t>t^*$ all laser energy goes to vaporization and we write, analogously to Eq. (12),

$$\rho\Lambda d(4\pi r^3/3)/d. \tag{28}$$

Integrating Eq. (28) from t^* to t we obtain the change in the radius of the particle in the process of vaporization

$$r(t)=r-\zeta(E-E^*)/4\rho\Lambda. \tag{29}$$

When

$$E=E_t=E^*+(4\rho\Lambda/\zeta)=E^*[1+(3\Lambda/cT^*)], \tag{30}$$

the particle is completely vaporized.

The arguments given above for determining the size of the vapor cloud for a flake are equally applicable to aerosol. Using these arguments, we write the following expression for the size of the vapor cloud of a vaporizing aerosol

$$R(t)=r[(\rho/\rho_v)\{1-[1-\zeta(E-E^*)/4\pi\Lambda r]^3\}]^{1/3}. \tag{31}$$

For $E=E^*$ the radius $R(t)=0$, and for $E=E_t$ the radius reaches its maximum value

$$R_m=r(\rho/\rho_v)^{1/3} \tag{32}$$

and corresponds to a completely vaporized aerosol particle.

2.6. Development of ionization

As mentioned above, the formation of SLP is a threshold effect, associated with the growth of ionization in a narrow range of laser-target interaction conditions. In order to describe this effect it is necessary to study the kinetics of ionization, taking into account its specific features in problems of this kind—closeness of a surface and presence of a high-frequency laser field.

Consider an element of volume located at a distance of the order of the radius of the focusing spot from the surface. Depending on the conditions of laser action, the volume can consist of vapors of the target material or a mixture of vapors with the surrounding gas. Electrons in this volume are heated by the high-frequency laser field. In most cases laser radiation is absorbed due to the inverse bremmstrahlung on neutral particles. The number of electrons with energies from ε to $\varepsilon+d\varepsilon$ present per unit volume due to this process is determined in the classical limit by the expression[73]

$$Q_f=\frac{\partial}{\partial\varepsilon}\{(8\pi e^2 q/3mc)[\nu_m/(p_m^2+\omega^2)\varepsilon^{3/2}]n(\varepsilon)/\varepsilon^{1/2}\}, \tag{33}$$

where $n(\varepsilon)$ is the electron energy distribution function, such that

$$\int_0^\infty n(\varepsilon)d\varepsilon=n_e,$$

n_e is the electron density, ν_m is the electron-neutral elastic-collision frequency, and ω is the frequency of the laser radiation. The electrons, taking energy from the laser field, give up energy in elastic collisions. The corresponding term in the equation for $n(\varepsilon)$ has the form[73,74]

$$Q_{el}=\frac{\partial}{\partial\varepsilon}(2m\nu_m\varepsilon n/M), \tag{34}$$

where M and n are the mass and concentration of heavy particles. Further, the kinetic equation contains the term $Q_{in}(\varepsilon)$, associated with inelastic electron losses to excitation and ionization. General expressions for it can be found in, for example, Ref. 75. Finally, in problems of laser breakdown electron losses caused by the spatial nonuniformity of the problem are found to be significant. There are significant difficulties in taking into account, in general form, the inhomogeneous terms in the kinetic equation. If, however, the electron density does not change much over the mean free path length or the size of the region of the field is much greater than the electron range, then the spatial nonuniformity can be taken into account by an approximate method.[73] Thus if electron diffusion is significant, the term

$$Q_d=-n(\varepsilon)\nu_d(\varepsilon), \tag{35}$$

where $\nu_d=\tau_d=D_eV/\Lambda^2, \mathscr{D}_e=v^2/3\nu_m=2\varepsilon/3m\nu(\varepsilon)$ is the diffusion rate-the inverse of the diffusion escape time of an electron from a volume with characteristic size Λ, must be added to the kinetic equation. Other cases when spatial transport must be taken into account will be discussed below. The kinetic equation for the function $n(\varepsilon,t)$ has the form

$$\partial n/\partial t=Q_f+Q_{el}+Q_{in}+Q_d. \tag{36}$$

Two approaches are mainly used at the present time to solve this equation. In the case of millisecond or longer laser pulses with characteristic rise time ~ 0.1 msec the high-frequency laser field grows relatively slowly. The average electron energies $\bar{\varepsilon} < \Delta$, I, where Δ and I are, respectively, the excitation and ionization potentials of the atom. Excitation (ionization) is realized by a small number of electrons, present in the "tail" of the quasistationary distribution function. The inequality $\tau_f \ll \tau_i$, where τ_f is the time over which a stationary distribution function is established and τ_i is the characteristic ionization time, holds. This means that the electron density remains virtually constant over times τ_f. The stationary solution of Eq. (36) for the kernel of the distribution function, neglecting the terms Q_{in} and Q_d, has the form[73,74]

$$n(\varepsilon) = C \exp\left[-(6m^2c/8\pi e^2 Mq) \int_0^{\varepsilon} d\varepsilon/(\nu_m^2 + \omega^2), \right. \tag{37}$$

where the constant C is determined from the normalization condition. In the case $\nu_m \sim v \sim \bar{\varepsilon}^{1/2}$ the well-known Margenau distribution ($\omega \neq 0$) and the Druivestein distribution ($\omega = 0$) follow from Eq. (33). Note that in a wide range the laser field can be considered to be high-frequency $\omega \gg \nu_m$. Then for any function $\nu_m(\varepsilon)$ we immediately obtain from Eq. (37) a Maxwellian distribution with the effective temperature

$$T_e = 4\pi e^2 Mq/3m\omega^2. \tag{38}$$

For example, for a CO_2 laser $\omega = 2\pi c/\lambda \approx 1.78 \cdot 10^{14}$ sec^{-1}, and the electron-argon elastic-collision frequency[73] $\nu_m \approx 5.3 \cdot 10^{12} p(\text{atm}) \cdot \text{sec}^{-1}$. Thus the inequality $\omega \gg \nu_m$ is satisfied well. For ruby and neodymium lasers the inequality holds even better. As the degree of ionization increases a term associated with the electron-electron collisions, which in turn maxwellizes the distribution function, must be included in the kinetic equation. Thus the stationary solution of the kinetic equation in a high-frequency laser field in the presence of elastic losses with both heavy and light particles is Maxwellian with the effective temperature (38). The deviations from a Maxwellian distribution can be associated with inelastic processes and with diffusion. Methods for calculating the distribution function in the case of a Maxwellian kernel and a non-Maxwellian tail are quite well developed and described in Ref. 75. We make use of some of them below.

When a target is exposed to microsecond laser pulses with a leading edge ~ 50–200 nsec the kinetic equation is solved by a different approach. The stationary solution in this case leads to very high average electron energies ($\bar{\varepsilon} \gg \Delta$, I), for which ionization is instantaneous. In reality, ionization occurs at the nonstationary stage, when an electron acquires in the high-frequency field sufficient energy for ionizing an atom. The ionization rate itself is determined by the growth time of the electron energy up to a certain value (usually this value is of the order of Δ). The equation for the average electron energy is obtained from Eq. (36) by multiplying by ε and integrating over the spectrum[73]

$$d\bar{\varepsilon}/dt = \varepsilon_m \nu_m - \delta \nu_m \bar{\varepsilon} - \bar{\varepsilon} \nu_d. \tag{39}$$

In Eq. (35) $\varepsilon_\omega = 4\pi e^2 q(t)/mc\omega^2$ is the average energy acquired by an electron, by means of the inverse bremmstrahlung, from the high-frequency laser field in a single collision with an atom and $\delta = 2m/M$ is the elastic-loss ratio. The ionization time is determined from the condition $\bar{\varepsilon}(t_i) \approx \Delta$. We shall assume that at the times t_i the characteristics of the laser radiation remain essentially unchanged. Then the solution (35) has the form

$$\bar{\varepsilon}(t) = \varepsilon_\omega \nu_m [1 - \exp(-t(\nu_d + \delta\nu_m))]/(\nu_d + \delta\nu_m). \tag{40}$$

From Eq. (40) we find

$$\nu_i = t_i^{-1} = (\nu_d + \delta\nu_m)/\ln[1 - \Delta(\nu_d + \delta\nu_m)/\varepsilon_\omega \nu_m]. \tag{41}$$

It follows from Eq. (41) that the development of ionization is possible only if

$$\Delta(\nu_d + \delta\nu_m)/\varepsilon_\omega \nu_m < 1. \tag{42}$$

The inequality (42) can be rewritten in the form

$$q \geqslant \Delta[(l^2/\Lambda^2) + \delta]/\varepsilon'_\omega. \tag{43}$$

where $\varepsilon'_\omega = \varepsilon_\omega/q$ and l is the electron mean free path. For a CO_2 laser $\varepsilon'_\omega = 2 \cdot 10^{-4}$ eV/(MW/cm^2). Substituting this value into Eq. (43) we find

$$q(\text{MW/cm}^2) > 1 \cdot 10^3 \Delta(\text{eV})(l^2/\Lambda^2 + \delta) V \tag{44}$$

In the case of irradiation of a smooth surface the diffusion length is $\Lambda \sim R$, and the radius of the focusing spot on a microononuniformity is of the order of the size of the vapor cloud of the evaporating microononuniformity. If it reaches the limiting value (12), then Eq. (44) will have the form

$$q_m = \pi^2 \Delta l^2/3\varepsilon'_\omega R_m^2. \tag{45}$$

In the preceding discussion diffusion was assumed to be electronic. This is valid at the initial stages of ionization development, when $R_D \gg \Lambda$, where R_D is the Debye radius. For $R_D \ll \Lambda$ diffusion becomes ambipolar and it plays a much less significant role.

3. FORMATION OF A SURFACE LASER PLASMA IN THE DIFFUSION REGIME IN VAPOR-GAS MIXTURES

3.1. Heating and vaporization of the surface as a whole

When the surface is irradiated with laser pulses with duration $\tau > 10^{-4}$ sec and characteristic rise time ~ 0.1 msec, microdefects on the surface are heated and vaporized with relatively low intensities of the laser radiation ($q < 1$ MW/cm^2). The electron temperature T_e is insufficient for ionizing the vapor forming due to vaporization of microdefects. An SLP does not arise until vaporization of the main mass of the target material starts. In vapor-gas mixtures the surface temperature T_w does not reach the boiling point of the target material T_b. In Refs. 11, 12, 23, and 59–68 the formation of SLP in vapor-gas mixtures was observed and investigated at the surface of different materials. Thus in Refs. 23 and 59–67 the intensity of the laser radiation was constant throughout the main interaction

time. The laser sources were a quasistationary CO_2 laser with rectangular pulses with duration (0.1–1.0) msec and power 1–10 kW (Ref. 60) and an experimental model of a technological cw CO_2 laser.[61] The focusing spots were (0.1–0.5) mm in size. The temperature of the irradiated sample was monitored continuously during the interaction.

Diagnostics methods with the required spatial and temporal resolution made it possible to measure the laser power, the intensity distribution in a focusing spot, the target temperature (pyrometry), and the plasma temperature (interferometry) as well as to study the dynamics of the spatial pattern of the process. The experiments were performed on metals and dielectrics (Zn, Pb, In, brass, steel, Ti, Ni, Al, Cu, Nb, Ta, W, Mo, C, Al_2O_3, SiO_2, Getinaks, and plexiglass) in air, nitrogen and its mixtures with oxygen, argon, helium, and xenon at pressures ranging from 0.01 to 1 atm. Similar investigations, but with less rich diagnostics, were performed in Refs. 11, 12, and 68 at the surface of different metals at pressures above atmospheric pressure. Atomic vapor-gas mixtures form in the atmosphere of inert gases at the surface of the metal. The electron temperature T_e in them is appreciably higher than the gas temperature T_g. The atmosphere of molecular gases N_2, CH_4, and air ($T_e \approx T_g$) consists of a molecular vapor-gas mixture. Breakdown of the vapor and the surrounding gas in some cases is observed for different values of the laser radiation intensity, and in other cases with one and the same value. Hysteresis effects are observed: The laser intensities required in order to maintain the plasma state can be lower than the values required for producing it. Surface laser plasma in vapor-gas mixtures was investigated theoretically in Refs. 69–82.

We first consider atomic vapor gas mixtures in which the electron temperature can decouple from the gas temperature. Two concepts of formation of SLP in atomic vapor-gas mixtures were formulated. The first concept, employed in most of the works indicated, is based on the assumption that the characteristic time over which the surface temperature changes as the surface is heated by laser radiation $\tau_m^{-1} = (\partial \ln n_m/\partial T)\partial T/\partial t$ is long compared to the characteristic diffusion time of the vapor $\tau_d \sim R^2/D_m$ or the ionization time of the vapor $\tau_i \sim (n_m\beta)_m^{-1}$. Here n_m is the vapor concentration, T is the vapor temperature, and β is the ionization factor. We now consider the concept in more detail.

3.1.1. Quasistationary model with a vapor cloud of limited size

In this case, for each value of the surface temperature there is a quasistationary distribution of vapor in space. The SLP forms mainly due to development of ionization in the vapor. Then the discharge spreads, with somewhat higher intensity, into the surrounding gas. In order to determine the time of onset of rapid ionization the equation of balance of charged particles, the energy of the charged particles, and the energy of the heavy particles must be formulated; this was done with one or another degree of detail in the works indicated. However, the moment of breakdown itself can be determined on the basis of simple criteria, which were discussed in the introduction. The discussion of this question given below mainly follows Ref. 82. Details can be found in Refs. 69–81.

First we write the stationary ionization condition for the vapor-gas mixture in atomic gas. Following Yu. P. Raizer's criterion,[56] we have

$$n_m\beta = \nu_d. \tag{46}$$

Since the vapor density is low, the gas density can be found from the condition that the pressure p is constant. The metal-vapor density decreases away from the target surface and is described by the diffusion equation. The calculations performed in Ref. 72 for a laser-heated sphere showed that n_m decreases slightly with increasing distance away from the surface and near the surface the temperature of the vapor $T \approx T_w$, where T_w is found from Eq. (3). We assume that the metal-vapor concentration in the region of the focus is constant and we determine it (in cm^{-3}) from the expression

$$n_m = AT^b \exp(-\Lambda/T). \tag{47}$$

In Eq. (47) T is expressed in electron-volts. The quantities A and b are constants, given for different metals, for example, in Refs. 83–84. The ionization coefficient β in the case of low electron temperatures T_e, when the "narrow location" lies in the region of excited states, is determined by the expression[58]

$$\beta = (2\Gamma\Lambda_1\Sigma_i/3\pi^{1/2}g_1)(\mathrm{Ry}/T_e)^3 \exp(-I/T_e)$$
$$= \beta^* \exp(-I/T_e), \tag{48}$$

where Σ_i is the partition function of a metal ion, g_1 is the statistical weight of the ground state of the metal atom, $\Gamma = 1.73 \cdot 10^{-7}$ cm^3/sec, $\Lambda_1 = 0.2$, and $\mathrm{Ry} = 13.6$ eV. In Eq. (46) $\nu_d = D_a/R'^2$, where D_a is the ambipolar diffusion coefficient.

We now write the temperature condition, which reduces to providing values of T and T_e such that the condition (46) is satisfied. We determine T from Eq. (3). This means that breakdown occurs prior to the RDV. This supposition is supported by the fact that there are no traces of fracture, noted in Refs. 63–65, of the target after laser action.

In order to determine T_e we employ the model with a vapor cloud of finite size.[78] This model is based on investigations performed in Refs. 72–80, where it is shown that, besides elastic losses, losses associated with heat conduction by electrons play a significant role in the balance of the electron gas. The role of heat conduction by electrons reduces to equalizing the electron temperature over some region of size R', where $R' = aR$ and R is the radius of the focusing spot. Due to the heat conduction by electrons the actual size of the region with hot electrons is somewhat larger than R and according to calculations[78] $a = 3.5$–4. Within the region of size R' the electron energy balance is determined by heating of the electrons in the laser field and elastic collisions. This leads to the following expression for the electron temperature:

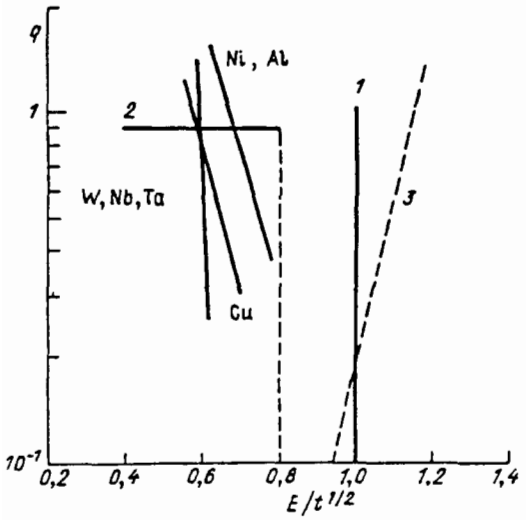

FIG. 3. Plane of the dimensionless variables $q-E/t^{1/2}$ for vapor-gas mixtures. The line *1* corresponds to heating of the target up to the boiling point, *2*—laser pulse from Ref. 83, *3*—boundary of RDV for Al, Ni, Al, and so on—boundary for the region of breakdown for Ni, Al, and other metals.

$$T_e=T+(\varepsilon'_\omega q/\delta), \tag{49}$$

where $\varepsilon'_\omega=[8\pi e^2(2-\zeta)/3mc\omega^2](R/R'^2)$.

The relations (3), (47), and (49) are necessary and sufficient conditions for breakdown. The intensity at which plasma of the vapors of the target material forms is found from these relations. We now transform to dimensionless quantities. In contrast to Eq. (6), however, we normalize the temperature, the ionization potential, and the vaporization energy to T_b i.e., $T'_e=T_e/T_b$, $T'=T/T_b$ and so on. It is convenient to introduce the following quantities for the energy, intensity, and time: $E'=E/E_v$, $q'=q/q_v$, $t'=t\chi/R^2$, where

$$E_v=\xi\rho cRT_b/\zeta, \quad q_v=\xi\rho c\chi T_b/\zeta R. \tag{50}$$

In dimensionless variables the equation for T (3) will have the form (the primes on the dimensionless variables are dropped)

$$T=E/t^{1/2}. \tag{51}$$

The electron energy balance (49)

$$T_e=(E/t^{1/2})+Bq, \tag{52}$$

where $B=\varepsilon_\omega c\rho\chi/\zeta\delta R$. Switching to dimensionless quantities in Eq. (46), using Eqs. (50) and (51), we find the relation between the threshold values of $E/t^{1/2}$ and q:

$$I/(Et^{-1/2}+Bq)+(\Lambda/Et^{-1/2})=\ln(AT^bT_e^b\beta^8/\nu_d). \tag{53}$$

Besides the explicit dependence on $E/t^{1/2}$ and q, the expression (53) depends on these quantities through T and T_e which appear in the argument of the logarithm: However, this dependence is weak.

We now display the dependences obtained in the plane of the dimensionless variables $q-E/t^{1/2}$ (Fig. 3). First we plot the vertical straight line (1) according to the equation $E/t^{1/2}=1$, corresponding to heating of the surface up to $T=T_b$. It is obvious that the lines corresponding to the boundary of the breakdown region must lie to the left of this straight line, since in the vapor-gas mixtures under consideration breakdown of the vapors should occur at temperatures $T<T_b$. The lines $q(E/t^{1/2})$ according to Eq. (48) are plotted in Fig. 3 for different metals. The values of q and $E/t^{1/2}$, lying to the right of these lines, correspond to the regimes of formation of SLP in vapors of the given material. Figure 3 also displays the experimental laser pulse (2) with threshold intensity q_{th}, constructed according to Ref. 65 for Al. It is evident that the boundaries of the breakdown regions for materials with such thermophysical properties (Ni, Al, Cu, Nb, Ta, W) with the given choice of dimensionless coordinates either merge or lie quite close to one another. The necessary thermophysical characteristics of the experimental materials and the computed[82] and experimental[66] values of the threshold intensities are presented in Table IV. As one can see, the latter quantities agree with one another; this indicates that the method is applicable for determining threshold quantities on the basis of the TC and IC.

In addition to determining the threshold values, the state of the plasma itself, forming as a result of the laser action, was investigated. It became clear that this plasma is a unique and interesting variant of a low-temperature, nonstationary, nonequilibrium, and spatially nonuniform

TABLE IV. Thermophysical characteristics of metals and thresholds for formation of SLP.

Metal	A, 10^{24} cm^{-3}	b	Λ, eV	I, eV	T_b, kK	ζ	χ, cm^2/s	Intensity at boiling q_b, MW/cm^2		Threshold intensity q_{th}, MW/cm^2	
								Calculation	Experiment	Calculation	Experiment
Ni	4,1	-2	4,5	7,6	3,2	0,04	0,4	5,5	>4	3,7	>4
Al	0,14	-2	3,3	6	2,8	0,04	0,5	4,9	4	3,8	3,8
Cu	3,85	-1,2	3,5	7,7	2,8	0,04	0,4	6,5	>4	4	>4
Nb	6,07	-0,3	7,5	6,9	5,1	0,06	0,2	5,8	—	3,1	—
Ta	16,4	-1	8,1	7,9	5,6	0,07	0,2	4,4	3,6	2,4	3
W	51	-0,5	8,7	8	5,7	0,06	0,2	5,9	>4	3,2	>4

plasma. The uniqueness is dictated by the heating with a low-frequency laser field, the presence of a surface supplying the vapor, the short duration of the laser action, the localization of the source of energy release in the focal region, and so on.

In these works[70–72] the problem was studied under the assumption that the vapor is in an ionization equilibrium (the vapor concentration is related to the electron concentration by Saha's formula with T_e). The authors assume that breakdown occurred when T_e reaches a sufficiently high value T^* (assumed equal to 10–15 kK). Further investigations showed, however, that a better description of the experimental data is obtained by considering nonequilibrium ionization. Ionization equilibrium can break down due to diffusion losses.[73–80] In the presence of diffusion losses and simultaneously ionization and recombination processes, associated with electron impact, the equation for the electron density on the beam axis has the form[75]

$$n_e=n_m[1+(n_e/K_m)+(1/n_e\beta_m(\tau_d)_m)]^{-1}$$
$$+n[1+(n_e/K)+(1/n_e\beta\tau_d F)]^{-1}. \qquad (54)$$

The first term in Eq. (54) corresponds to a stationary nonequilibrium concentration of vapor ions. The vapor quantities are marked with a suffix m. The second term corresponds to gas ions (no suffix), and n is the concentration of gas atoms. In the derivation of Eq. (4) it was assumed that ionization and recombination are caused by collisions with electrons, so that $\alpha=\beta/K$, where α is the ionization coefficient and K is the ionization equilibrium constant. The function F takes into account the possible deviation from a Maxwellian electron distribution at high energies in the kinetics of ionization of the main gas.[58] Figure 4 displays the function $n_e(T_e)$ calculated from Eq. (54) for a mixture of argon and titanium vapor for the experimental conditions of Ref. 63: $p=1$ atm and $T_w=0.25$ eV. The curve 1 in Fig. 4 corresponds to ionization equilibrium. The curve *2* corresponds to $\tau_d=0.4$ sec ($R=2$ cm) and the curve *3* corresponds to $\tau_d=0.4\cdot 10^{-3}$ sec ($R=0.02$ cm). It is evident that the form of the nonequilibrium function $n_e(T_e)$ is qualitatively different from that of the equilibrium function. The latter function is monotonic and contains no sections of rapid growth, which can be interpreted as breakdown. Several states of SLP can be separated in the nonequilibrium function. For low values of T_e volume ionization is inefficient and cannot compensate diffusion losses. The electron density will be determined by diffusion in the zone of heating of electrons produced due to thermal ionization of the vapor at the temperature of the surface. In this diffusion regime, in order of magnitude, $n_e\sim(n_mK_m)^{1/2}$. This quantity is marked in Fig. 4 by the dashed line. As T_e increases, the ionization efficiency increases extremely rapidly and when some threshold value T_A is reached a practically abrupt transition occurs from the diffusion regime to a regime with volume ionization of the metal vapors (the branch AB). The threshold value T_A is determined from the condition

$$n_m\beta_m(\tau_d)_m\geqslant 1.$$

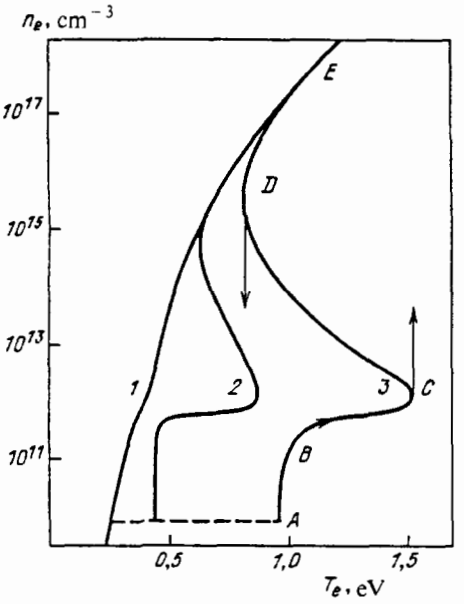

FIG. 4. $N_e(T_e)$, calculated from Eq. (54) for a mixture of argon and tantalum vapor in application to the experimental conditions of Ref. 80.

As T_e increases further (the branch BC), n_e increases continuously owing to increasing degree of ionization of the vapors. At the point C ionization of the main gas starts. Here

$$n\beta\tau_d F\geqslant 1. \qquad (55)$$

The quantity $F\sim 1$, since it is determined by the relatively low value of n_e at the point C. Subsequently, as n_e increases due to ionization of the main gas, the criterion (55) holds for lower values of T_e. As n_e increases, T_e decreases (the branch CD). At the point D the quantity $F\approx 1$ and for this reason $n\beta\tau_d\geqslant 1$. Further, n_e changes according to the equilibrium function (the branch DE). It is easy to show that the descending section DC is unstable. For this reason, in reality, when the plasma reaches the point C it abruptly switches into the state E with significant ionization of the main gas. This transition is marked by an arrow in Fig. 4. If, however, while in the state E the temperature T_e is now decreased, n_e will vary according to the stable branch ED. At the point D the plasma jumps abruptly into a state with much lower values of n_e. In addition, if for the curve *2* this is a transition into a state with ionized vapors, then for the curve *3* it is a transition to the diffusion state. It is evident that in the latter case $T_D<T_A<T_C$. The temperature at which the discharge in the main gas is extinguished can be lower than the ignition temperature T_A of a discharge in the vapor and the ignition temperature T_C of the discharge in the main gas. This behavior was observed in Ref. 80.

The qualitative principles following from Eq. (54) were confirmed by more detailed calculations in Refs. 96–100, where the equations of balance of the number of electrons and the energy of the electrons were written in a cylindrical geometry for an atomic gas with an admixture of vapor of a metal irradiated with a laser beam. It was shown that the temperature and density of the electrons on

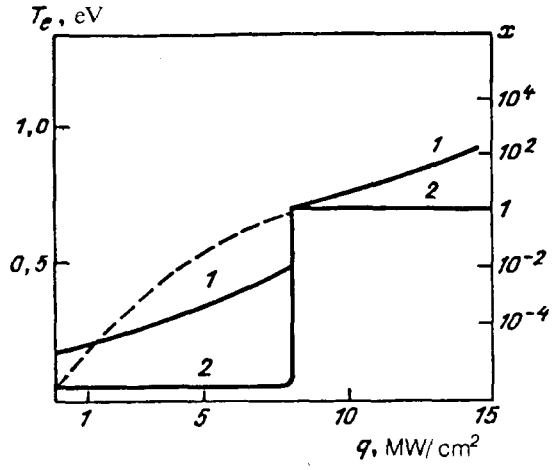

FIG. 5. T_0 and x on the axis of a laser beam at a tantalum surface in an argon atmosphere as a function of the intensity. *1*—T_0, *2*—x (degree of ionization of the vapors).

the laser beam axis have, as a function of the intensity, a break at a certain value of the intensity. In Refs. 96 and 97 this was done by solving these equations numerically and in Refs. 98 and 99 the equations were solved by an approximate analytical method. The numerical results of Ref. 96 are displayed in Fig. 5. Argon with an admixture of tantalum vapor $n_{Ta}/n_{Ar}=1.5\cdot 10^{-5}$ with $T=0.175$ eV and a pressure of 1 atm was studied. The radius of the laser beam was $R=0.06$ cm. For low values of q the degree of ionization is low and remains virtually constant right up to the breakdown values $q=8.2$ MW/cm^2. After this the temperature and degree of ionization grow in a jump-like manner. The degree of ionization changes by six orders of magnitude, reaching the state of complete ionization of the vapor. Both the pre- and post-breakdown temperatures T_e grow linearly, and at the moment of breakdown T_e undergoes a jump.

3.1.2. Nonstationary model

In this model the time τ_m is assumed to be short compared to the diffusion or ionization times. This means that there is not enough time for the vapors leaving a surface of area πR^2 to penetrate significantly into the surrounding gas. In the equations for n_e and T_e the terms describing spatial transfer are no longer important. Such a system was solved numerically in Ref. 97 under this assumption. A tantalum target in argon with $p=1$ atm and $R=0.2$ mm was studied. The computational results are displayed in Fig. 6. We note that Fig. 6a corresponds to the prebreakdown situation, while Fig. 6b corresponds to breakdown at the end of the laser pulse. We shall discuss the time dependence of the principal characteristics of SLP. As is evident from Fig. 6, the temperature of the surface increases slowly in both cases. The vapor concentration n_m (here and below the concentration of heavy metal particles) changes by many orders of magnitude. By the end of the pulse we have in the case a $n_m\sim 10^{11}$ cm^{-3}. In the case b we obtain

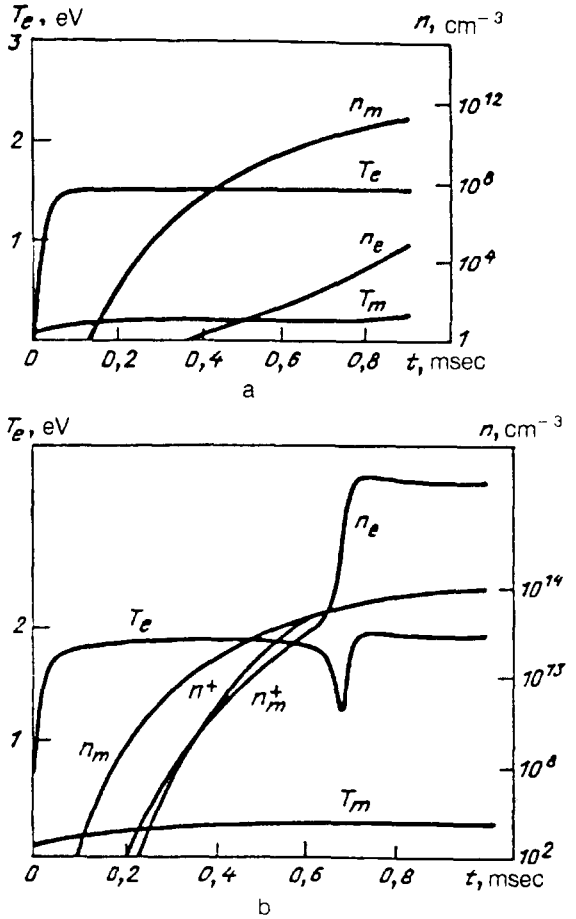

FIG. 6. Time dependence of the parameters of SLP for a tantalum target in argon and $q=2$ MW/cm^2 (a) and 2.6 MW/cm^2 (b).

$n_m\sim 10^{14}$ cm^{-3}. The time dependence of T_e is interesting. The temperature T_e reaches within a very short time a quasistationary value, which, initially, while there is little vapor and no ionization losses, is determined by heating by the laser radiation and other losses. When $q=2$ MW/cm^2 this situation remains up to the end of the pulse and $n_e\ll n_m$. Some increase in n_e is observed only at the very end of the pulse. In the case b $n_m\approx n^+$ from the very beginning of the process, though the ionization potential of tantalum is appreciably lower than that of argon; the tantalum vapor concentration is low enough to ensure that this equality holds. It is evident that n_m^+ and n^+ grow more rapidly than n_m and at some time they are equal to n_m. At this moment the ionization losses become important in the energy balance of the electron gas, T_e drops appreciably, and the concentrations n_m^+ and n^+ grow rapidly—breakdown occurs. After breakdown the ionization losses are compensated by the opposite process and T_e grows once again. Breakdown of the gas and vapors occurs virtually simultaneously. This is confirmed by the experimental data,[84] obtained for close values of the parameters. The quasistationary and nonstationary models are in this sense alternative models. The first one is valid under conditions when the diffusion time is much shorter than the time over which the density of the metal vapor changes and the sec-

ond model is valid in the opposite case. Both situations can be realized under real conditions. Thus in Ref. 84 with $I=0.25$ mm breakdown of the vapors and the surrounding gas occurs for $q=3$ MW/cm^2, which agrees with the results of the nonstationary model. When the radius of the focal spot decreases to 0.1 mm, the diffusion time becomes significantly shorter, since $\tau_d \sim R^2/D$, and the ratio of the characteristic times shifts in favor of the quasistationary model. In Ref. 84 a difference appears in the breakdown intensity for Ta and Ar, as is typical for the quasistationary model.

We now consider the characteristic features of the formation of SLP in *molecular* vapor-gas mixtures. In such mixtures, besides the small decoupling of T_e from T, noted above, the composition is more complicated and correspondingly the ionization kinetics is more complicated. As in the case of atomic gases, breakdown is initiated by development of ionization in metal vapors, which consist of an impurity in a molecular gas. In Ref. 90 it was assumed that ionization equilibrium exists and the vapor concentration in the region of the focus is approximately constant. In this case the problem reduces to solving the heat-conduction equation with an exponentially time-dependent heat source. For a spherically symmetric geometry this is equivalent to the problem of asymmetric inflammation or ignition of a hot surface.[103] The threshold value obtained for q in this approach is virtually independent of the properties of the surrounding gas (q is virtually independent of p and $q \sim 1/R$). In the experiment of Ref. 81 other dependences were recorded ($q \sim p^{-1/2}$ and $q \sim 1/R^2$). In a thermal explosion the temperature of the medium increases rapidly and the vapor and the surrounding gas are ionized virtually simultaneously, so that on the basis of this model breakdown in the vapors is indistinguishable from breakdown in the main gas.

Breakdown of vapors in a molecular gas was studied on the basis of nonequilibrium ionization kinetics in Refs. 94 and 99. In a molecular vapor-gas mixture $T_e \approx T$. This requires that over the time τ_m the energy of the laser radiation must be converted into the translational energy of the molecular gas. This is possible if the electron-to-molecular gas energy transfer time τ(e-m) and the vibrational-translational energy exchange time τ(m-m) are short compared to τ_m and τ_d. For molecular nitrogen under the conditions of the experiment of Ref. 75 with $p=1$ atm, $R=0.2$ mm, and $D \sim 10$ cm^2/sec the characteristic times of the problem are: $\tau_m \sim 5 \cdot 10^{-4}$ sec, $\tau_d \sim 4 \cdot 10^{-5}$ sec, $\tau(\text{e}-\text{m}) \sim 10^{-9}-10^{-10}$ sec, $\tau(\text{m}-\text{m}) \sim 10^{-5}$ sec. Thus the condition for the mixture to have a single temperature is satisfied.

The ionization condition has the form (46) with $\tau_d = R_d^2/D_a$, were R_d is the characteristic diffusion radius, which depends on the temperature profile. In order to obtain the thermal condition it is necessary to study the equation of balance of the gas temperature. Under the assumptions made above, all of the energy of the laser radiation goes into heating of the gas. Losses are associated with the heat conduction of the gas, so that

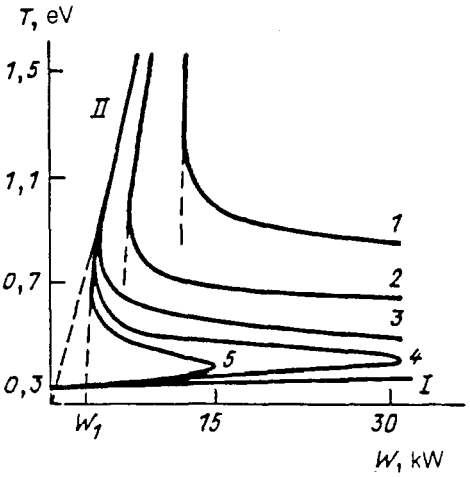

FIG. 7. Temperature on the laser beam axis at the tantalum surface in molecular nitrogen as a function of the power.

$$-\nabla(\varkappa \nabla T) = \varepsilon'_\omega q \nu n_e, \tag{56}$$

where $\varkappa$ is the thermal conductivity of the molecular vapor. The solution of Eq. (56) must be found under the condition (46), when electron losses due to diffusion are equal to electron production by volume ionization. Due to the extremely sharp temperature dependence of the ionization rate, when the intensity exceeds by a small amount the value determined from Eq. (46), ionization and recombination processes predominate over diffusion. The electron density in this case is determined from the equation $n_e = (n_m \beta/\alpha)^{1/2}$, where α is the recombination coefficient. The latter relation, if the ionization and recombination kinetics are determined by collisions with electrons, leads to the Saha formula. Indeed, in this case, $\beta/\alpha = K^{-1}$, where $K = h^3 \Sigma_a \exp(-I/T)/(2\pi m T)^{3/2} \cdot 2\Sigma_i$ is the ionization equilibrium constant, and Σ_a and Σ_i are the partition function of an atom and ion of the metal vapors. Equations of the type (56) with an exponentially temperature-dependent heat source together with an equation for electron balance, in which ionization-recombination and ambipolar diffusion processes were taken into account in a cylindrical geometry, were solved in Ref. 99. Trial functions were employed for solving the problem. A mixture of tantalum vapors and molecular nitrogen at a pressure of 1 atm was studied. The mixture was irradiated with CO_2-laser radiation. The results are displayed in Fig. 7 and 8. In Fig. 7 the temperature T on the beam axis is plotted as a function of the laser power for different focusing spot sizes $R=0.015$ mm (curve *1*), 0.03 (2), 0.3 (3), 30 (5), and larger. It is evident that these S-shaped curves fall between two lines. The first line (I) corresponds to $n_e = n_w$, where n_w is the equilibrium electron density with $T = T_w$ (T_w is the temperature of the surrounding medium). The second one (II) corresponds to $n_e = n_M$, where n_M is the metal vapor concentration. Increasing the beam radius is equivalent to decreasing the role of ambipolar diffusion in nonequilibrium ionization. It results in a de-

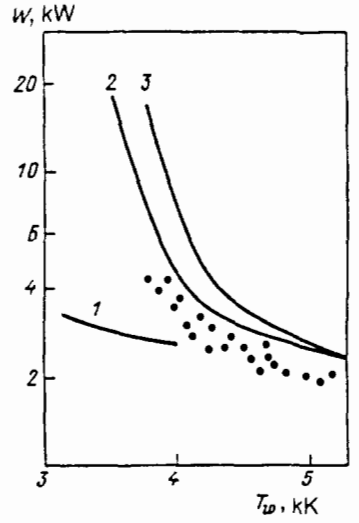

FIG. 8. Breakdown power of vapors in nitrogen as a function of the surface temperature. Dots—experimental data of Ref. 81 for Ta; solid lines—calculations of Ref. 95 for $p=1$ atm; $R=1.5\cdot10^{-2}$ cm; *1*—Nb, Mo; *2*—Ta; *3*—W.

crease of laser power, at which the system can exist in two uniform states. The ionization of the metal vapors reaches equilibrium when $R\geqslant3$ cm.

In Fig. 8 the computed breakdown power W (Ref. 86) is compared to the experimental data of Ref. 81. It is evident that there is agreement with respect to the dependence of W on the temperature of the metal surface. The dependence of W on the type of metal also agrees with the experiment. This correlation is determined by the quantity $\Lambda/T_w+I/T$; this confirms the proposed concept of breakdown for molecular gases.

3.2. Heating and vaporization of aerosol particles

According to the logic of our exposition, we should describe the results on the initiation of SLP by heating and vaporization of microdefects of the surface in the diffusion regime. In contrast to aerosol particles, however, we do not have now any experimental results that confirm such a possibility, so that we shall describe cases when the plasma is initiated by heating and vaporization of aerosol particles in the diffusion regime.

Such a situation is realized with a low-threshold collective optical breakdown in a gas (LCOB) with suspended aerosol particles. Such breakdown arises as a result of the heating of particles by the laser beam, vaporization of the particles, and formation of a plasma cloud as a result of merging of microflames from separate particles.[104–108] Vaporization of the particles occurs, as a rule, at a temperature below the boiling point, so that the plasma cloud is a vapor-gas cloud. Development of ionization is facilitated by the fact that the plasma cloud is large compared to the vapor-gas cloud from a separate particle. In the presence of LCOB breakdown intensities are very low and reach values of 0.2–5 MW/cm^2.

In order for RDV to be realized in the diffusion regime (region in Fig. 2) it is necessary that $T^*\leqslant T_b$. Using Eq. (27) this inequality can be rewritten in the form

$$r\geqslant\zeta(A\Lambda/RT)E/4\rho\Lambda V. \tag{57}$$

On the other hand, RDV is valid if $q<q^*$. The latter inequality can also be rewritten as a limit on the particle size:

$$r\geqslant(\zeta E/4\rho\Lambda)\ln(4\rho\Lambda v_0/q\zeta)V. \tag{58}$$

The strongest of the inequalities (57) and (58) must be chosen. Thus under the experimental conditions of Ref. 100 $q\approx1$ MW/cm^2 and $E\approx500$ J/cm^2. For Al the inequalities (52) and (53) hold for $r\geqslant30$ μm. LCOB was observed for Al particles with $r=80$ μm; this indicates that the RDV is realized in the diffusion regime.

The development of ionization in a vapor-gas mixture, formed by the overlapping clouds of separate particles vaporizing in the surrounding molecular gas (air), is similar to that studied in Sec. 3.1. The temperature of the mixture is determined from the balance of the absorbed laser energy and the losses associated with heat conduction. Thus in Ref. 110 a condition obtained by studying a slow-combustion wave was formulated for this.[73] Besides absorption of laser energy, associated with inverse bremmstrahlung, another mechanism was proposed in Ref. 110. This mechanism is associated with absorption of radiation by extremely small droplets of a condensed phase (clusters), present in the vapor at temperatures below the saturation temperature T_s. These assumptions enable explaining in part the experimental data of Ref. 104, though there is some discrepancy for small particles with $r<10$ μm. This discrepancy could be connected with a transition to the hydrodynamic regime of vaporization of such particles. We shall examine this regime in the next section.

4. PLASMA FORMATION IN THE HYDRODYNAMIC REGIME IN THE PRESENCE OF AN EROSION FLAME

Historically breakdown near the surface of irradiated materials was first investigated under conditions when RDV was realized when the surface temperature was higher than the boiling point of the material. A vapor jet, in which the pressure is higher than the pressure of the surrounding gas, is formed.[2,3,19] The appearance of the SLP was explained within the so-called vaporization or thermal model.[3,19,25,26,109–120] According to this model, breakdown occurs due to the development of an electron avalanche in the jet of dense vapors. This actually requires that the ionization condition, studied in Sec. 2.6, be satisfied. As is clear from what has been said above, it must be supplemented with the thermal condition, adequate for the vapor efflux regime being considered; this will be done below. In Refs. 35 and 36 breakdown in vapor was regarded as a "flash of absorption" in dense vapors heated in an equilibrium fashion by the laser radiation. As the thickness of the vapor layer at the surface increases, cooling of the gas due to expansion decreases and becomes equal to the heating due to absorption of laser radiation by the vapor and condensate particles; the temperature increases locally and grows rapidly due to the nonlinear temperature depen-

dence of the absorption coefficient of the vapors. The degree of ionization of the vapor grows at the same time. There appears a "flash" of absorption and a flash, in the direct sense of this word, of radiation due to a sharp increase in the luminosity of the vapor, and breakdown of the vapor occurs. This model is limited to conditions when the degree of ionization can be regarded as having the equilibrium value.

Somewhat singular are models in which the main mechanism of formation of SLP is avalanche ionization in the gas layers adjoining the target; the threshold of the avalanche ionization is reduced by electron emission from the target[121] and preheating of the gas by a shock wave excited by ejection of target material.[122] In Ref. 121 different materials were irradiated with a CO_2-laser pulse in air. Metals reduce the breakdown threshold most strongly. In addition, metals, capable of being heated up to high temperature without transforming into a different phase state, give more efficient thermionic emission, giving rise to a greater reduction of the breakdown threshold. An assessment of the effect of an increase in the electron density near a surface on the reduction of the breakdown threshold was made in Ref. 19. Thus when the electron density increases from 1 cm^{-3} up to 10^{14} cm^{-3}, the breakdown threshold intensity is reduced by a factor of 4.5. At the same time, in Ref. 121 the threshold was one or two orders of magnitude lower, depending on the type of material, than the threshold of breakdown of pure air. Thus an increase in the initial electron density due to thermionic emission from the target surface cannot explain the experimentally observed breakdown thresholds. In Ref. 122 it was assumed that under the action of laser radiation a layer of matter with a thickness of the order of the absorption depth of the radiation in the target material is ejected from the target surface. This layer then acts like an accelerating piston and creates a shock wave in the surrounding air. The air is preionized, after which an electron avalanche can develop under the action of the laser radiation.

In spite of the difference in the models and approaches, the threshold and appearance of SLP can also be determined in erosion flames with the help of adequately written thermal and ionization conditions.

4.1. Heating and vaporization of the surface

In Refs. 80–84, where the action of millisecond laser pulses on the surface of different materials was investigated, it was found that in many cases hydrodynamic regimes are realized in addition to diffusion regimes. The characteristic states of plasma found in Ref. 84 are displayed in Figs. 9a–c. Figures 9d–g show the recorded oscillograms of the intensities of the characteristic emission lines of the plasma, illustrating the dynamics of the spectral composition of the emission. For many materials optical breakdown is preceded by an erosion flame of the products of decomposition of the material. The flame is oriented perpendicular to the target surface, irrespective of the direction of incidence of the radiation (Fig. 9a). The emission spectrum of the flame consists of the sensitive lines of atoms and bands of molecules of the target material

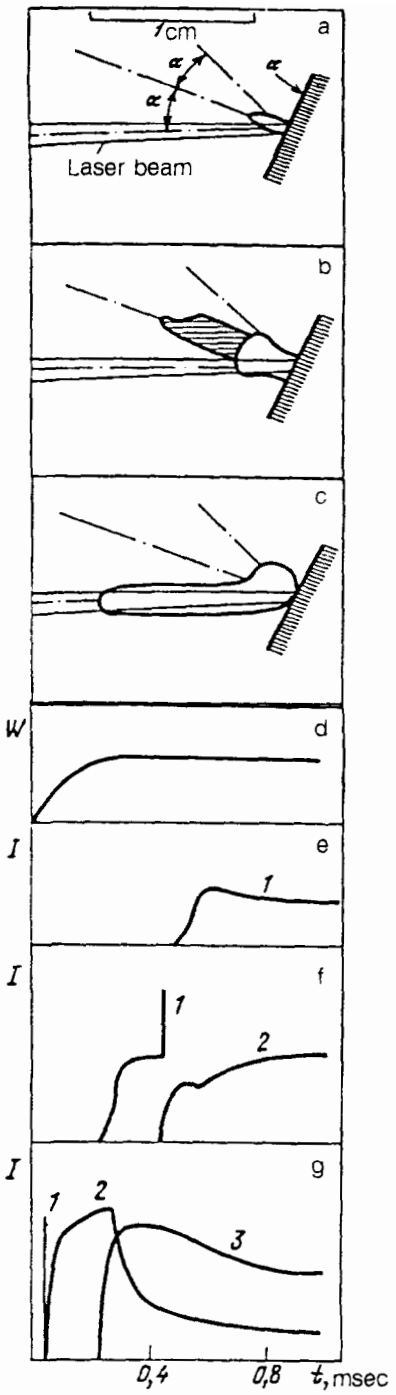

FIG. 9. Schematic diagram of states of SLP near a Ti surface. a—erosion flame in air (W=2 kW). b—optical discharge in vapors in air (W=6 kW). c—optical discharge in gas in argon (W=6 kW). d–g—oscillograms of signals from detectors of radiation intensities; *1*—integrated emission; *2*—Ti 115129 cm^{-1} line; *3*—Ar 114619 cm^{-1} line; d–f—for Figs. a–c; d—time dependence of the laser power.

and compounds formed with the surrounding gas (Fig. 9e). As the intensity increases, optical breakdown of the target vapors occurs and is accompanied by formation of a different state of the SLP—an optical discharge in these vapors. This state is characterized by the appearance of an asymmetric "branch" of plasma in the direction of the incident laser beam (Fig. 9b). The emission spectrum of

the optical-discharge plasma in the vapors consists of lines and ions of the target material (Fig. 9f); the region where ion lines are seen is concentrated in the waist of the laser beam. As the radiation power is increased further, the plasma passes into a new state—plasma of an optical discharge in the gas. The optical discharge in the gas extends along the laser beam (Fig. 9c), moving significantly away from the target surface. Plasma also exists in the beam reflected from the target surface, but its emission is weaker. The lines of the gas ions become the strongest lines in the emission spectrum of such a plasma (Fig. 9g).

It should be noted that as the radiation power increases, the above-described sequence of different states (erosion flame—optical discharge in vapors—optical discharge in gas) can break down in the case of a metal with high reflectivity and thermal conductivity (Cu, Al) or refractory metals (W, Ta, and others), i.e., when heating of the irradiated surface is impeded. In this case the optical-discharge plasma can arise before the appearance of an erosion flame in the diffusion regime (see preceding section).

The parameters of SLP in different states are significantly different. Investigations of the spectral characteristics of an erosion flame have established that the flame is a jet of vapors of the target material with temperature close to the boiling point of the target material.[83] An erosion flame is a jet of vapors of the target material that is transparent to CO_2-laser radiation and does not influence the effectiveness of the interaction of the radiation with the material. The parameters of SLP depend on the target material and the gas and change comparatively little with increasing laser power within a single state. The temperature of the discharge plasma in the vapors was, under the conditions of the experiment, $T\approx 8$–12 kK on the discharge axis near the target and rapidly drop away from the axis. The maximum temperature of the discharge plasma in the gas was $T\approx 20$–24 kK. The electron density in the discharge in metal vapors and in gas fell into the range $n_e\approx(1\text{–}5)\cdot 10^{17}$ cm^{-3}.

Near the surface of *easy-melting metals*, which have relatively low boiling points (Pb, Zn, In), breakdown of an erosion flame of metal-atom vapors occurs for laser radiation intensities only slightly higher than the value required for formation of the flame.[23] The breakdown intensities in this case lie in the range 0.5–3 MW/cm^2. The concept of breakdown for these conditions was proposed in Ref. 123.

In contrast to the metals, which we considered, with relatively high values of T_b, when thermal ionization at the surface gives quite high values of the initial electron density, the values of T_b for the group of easy-melting metals being considered are low and the corresponding electron density is very low. In this case $r_d > R$, so that at the first stage of heating diffusion is purely electronic ($\tau_d\approx R^2/D_e$). For surrounding-gas pressure ≈ 1 atm, $R\sim 10^{-2}$ cm, and $t_d\approx 10^{-8}$ sec. In order for an avalanche to develop it is necessary that $\nu_i \geqslant \tau_d^{-1}$, where ν_i is the ionization rate. Here we call attention to a specific mechanism of ionization under the conditions being considered. Electrons heated by the laser field lose energy in elastic collisions. Thus for $q=0.5$–3 MW/cm^2 an estimate of T_e from Eq. (44) gives $T_e\approx 1.5$–2 eV, which is somewhat higher than T_w. Due to the high values of T and the high gas density $n\sim 10^{18}$–10^{19} cm^{-3} every electron whose energy reaches $\varepsilon\sim I$ instantaneously ionizes an atom. The ionization rate is determined by the number of electrons which, due to diffusion along the energy axis, enter the region $\varepsilon\sim I$. In addition, in this case diffusion occurs as a result of collisions between electrons and atoms. The ionization rate can be calculated by the "infinite sink" approximation[75]

$$\nu_i=\delta\nu(I)I^{3/2}\exp(-I/T_e)/T_e^{3/2}, \tag{59}$$

where $\nu(I)$ is the electron-atom elastic-collision frequency for electron energies $\varepsilon\sim I$. According to Eq. (59) $\nu_i\sim 10^6$ sec$^{-1} < \nu_d$, so that as long as $T < T_b$ ionization does not occur. As soon as $T > T_b$ a transition occurs into the regime of jet evaporation. The vapor pressure and density in the jet grow rapidly with increasing T. The frequency of elastic collisions of electrons, which is now determined by collisions with vapor atoms, and the ionization rate ν_i also increase. The diffusion-loss rate $\sim 1/n_m$ drops. For a pressure of the order of several atmospheres $\nu_i\sim\nu_d\sim 10^6$ sec^{-1}. The velocity of the jet in the gas becomes close to the velocity of the jet in vacuum. The form of the losses changes—convective removal of electrons in the jet with characteristic time $\sim R/v\sim 10^{-7}$ sec now predominates (v_v is the speed of the jet, equal in order of magnitude to the sound speed v_s). Thus breakdown requires that over the period of time that the vapor transverses a characteristic distance $\sim R$ the electron density must increase from the initial low values n_i (of the order of 1 cm^{-3}, which can be determined by the background radioactivity) up to quite high values n_f. The value of n_f can be taken as the electron concentration at which the rate of energy exchange as a result of elastic collisions with atoms is equal to the electron-ion collision frequency. When $n_e\sim n_f$, further development of ionization occurs very rapidly and the vapor instantaneously becomes highly ionized. The nonstationary ionization condition has the form[73]

$$\ln(n_f/n_i)\nu_i^{-1}=R/v. \tag{60}$$

In order for the criterion (60) to be satisfied, the vapor concentration n_m and the expansion velocity v must have definite values, and these values in turn depend on the surface temperature T_w—the thermal condition. Assume that by the time of the transition to the jet evaporation stage, the RDV holds, i.e., $T^* \geqslant T_b$. Then Eq. (13) can be used for the vaporization of a surface layer of thickness d. Dividing Eq. (13) by $t-t^*$ and using the law of conservation of mass $\rho v=\rho_v v_v$, we obtain

$$n_v u_v\Lambda=\zeta(E-E^*)/(t-t^*). \tag{61}$$

The quantity $v_v\approx(1-\varphi)(T_v/2\pi M)^{1/2}$, where φ is the particle reflectance of the surface, is close to the velocity at which the vapors expand into the vacuum.[18] Due to the presence of the Knudsen layer the temperature T_v in the vapor jet is related to the surface temperature T_w by the relation[18] $T_v=0.67T_w$. The pressure in the jet can be ex-

TABLE V.

	R = 0.1 mm								R = 0.25 mm				
	T_b	I	Λ	q_b	q э	q р	T_w	n_v	$>q_b$	q э	q р	T_w	n_v
Zn	0,102	9,4	1,2	2,2	3,4	3,3	0,13	9,9	0,7	1,0	1,	0,13	9,0
Pb	0,175	7,4	2,0	0,7	1,3	1,2	0,2	3,9	0,3	0,7	0,7	0,2	3,4
In	0,202	5,8	2,5	1,9	2,6	2,9	0,27	4,5	0,8	1,2	1,3	0,26	2,3

pressed in terms of the saturated-vapor pressure similarly to Eq. (42). As a result, the maximum intensity at which breakdown occurs in the vapor jet can be found from Eqs. (60) and (61). The computed values of q, together with the initial data and the experimental results, are given in Table V. In Table V T_b, I, and λ are expressed in eV, n_v is expressed in 10^{19} cm^{-3}, q_b and q are expressed in MW/cm^2, e designates the experiment of Ref. 23, r designates the calculations given in Ref. 123, and q_b is the intensity at which an erosion flame forms. It is evident that the computed values agree with the experimental values. As the radius R increases, the values of q decrease. This is connected, on the one hand, to the decrease in the intensity q_b at which the temperature at the center of the focusing spot at the end of the pulse reaches the boiling point and, on the other, to the increase in the transit time over the characteristic distance $\tau \sim R/v_v$. High particle densities of the order of 10^{19}–10^{20} cm^{-3} are reached in jets; this justifies the application of the equation for evaporation into vacuum.

In the case of the action of laser radiation on nonmetallic substances, in contrast to easy-melting metals, with high absorption coefficient and low thermal conductivity (C, Al_2O_3, SiO_2, plastics, and so on) the flame breakdown intensities are significantly higher than the intensities required for formation of a flame.[23] Thus for graphite at atmospheric pressure a vapor jet forms for $q \geqslant 0.5$ MW/cm^2 and $T_w = T_b = 4100$ K.[23] Breakdown of vapor is also observed with $q = 17$ MW/cm^2, $T_w = 5000$ K, and $R = 0.1$ mm. In this case the erosion flame consists of a dense molecular vapor. Ionization cannot develop in it. The estimates made in Ref. 124 showed that the absorption of laser radiation, associated with inverse bremmstrahlung on atoms and ions, cannot give the breakdown intensities required in the experiment. In a dense molecular vapor the absorption spectrum consists of many strongly broadened overlapping vibrational-rotational lines, which form a quasicontinuum. Direct absorption of laser radiation by the vapor molecules is very likely. The absorption coefficient can be represented as $\zeta = a\rho_v$, where a is a constant. The absorption cross section is of the order of $\sigma \sim 10^{-19}$ cm^2. This value is characteristic for molecular absorption.[125] As a result of this, vapor is heated and ionized. When the degree of ionization is high enough, other mechanisms of absorption of laser radiation come into play (for example, inverse bremmstrahlung). The absorption now depends strongly on the degree of ionization. In such a situation an ionization-thermal explosion, associated with breakdown, is possible under further heating.[73]

We shall now find the conditions under which heating of the molecular gas due to absorption of radiation becomes significant. We write down in the one-dimensional approximation the law of conservation of energy per unit mass of vapor, moving with velocity u along the x-axis perpendicular to the surface of the body $\rho u d[h + u^2/2]/dx = \sigma n_v q$; here $h = \gamma/(\gamma - 1)kT/Nm$ is the specific enthalpy of the vapor and N is the number of atoms per molecule. The motion of the jet can be assumed to be one-dimensional over a distance of the order of R. Obviously, if over a distance of the order of R from the surface the change in the enthalpy flux becomes of the order of the flux itself, then significant heating of the jet will occur, and for this reason

$$u(h + u^2/2) \approx \sigma n_v q R. \tag{62}$$

Since the vapor pressure near the surface is significantly higher than the pressure of the surrounding gas, the velocity u is close to the local velocity of sound $u = (\gamma kT/Nm)^{1/2}$. The vapor temperature can be expressed as $T_v = 0.67T_w$—the condition for the flow to pass through the Knudsen layer.[18] For carbon and a CO_2 laser, setting $T_w = 0.43$ eV and $R = 0.1$ mm, we obtain from Eq. (62) $q \approx 14$ MW/cm^2. In the experiment of Ref. 23 breakdown occurred under analogous conditions for $q = 17$ MW/cm^2. According to Eq. (57), q decreases with increasing R. This also agrees with the experiment of Ref. 23. This mechanism of breakdown is described in greater detail in Ref. 126. For small distances from the surface, a one-dimensional problem of supersonic vapor flow was solved, taking into account absorption of laser radiation. At large distances, where the flow is three-dimensional, absorption of laser radiation was neglected. The parameters of the vapor behind the front of the stationary shock wave—"suspended shock"—were determined from the results of the solution of the one-dimensional problem and the intensity of laser radiation at which ionization-thermal explosion was possible was found. The obtained intensities are close to the experimental values.

Breakdown of metal vapors under intense vaporization of metal surfaces irradiated with neodymium laser pulses with duration ~ 1 μsec and intensity $\sim 10^8$ W/cm^2 was studied in Ref. 127. Among other factors, characteristic for RDV, such as, decrease of the reflectance of the metal and

TABLE VI. Characteristics of metals and surface temperature at the moment of breakdown ($q=380$ MW/cm^2, $R=0.07$ mm).

metal	A, eV	M, amu	T_b, K	Temperature at breakdown, K	
				calc	Exp.
Ni	4,7	59	3200	3480	3500
Al	4,1	27	2800	3390	3200
Cu	4,8	64	2800	3000	3100

formation of an opening in the sample, it was confirmed that the temperature of the surface at the moment of breakdown is virtually independent of the intensity of the incident radiation. It is constant for each material and several hundreds of degrees higher than the boiling point. In Ref. 127 it was assumed that the heating of the surface up to temperature T_b is satisfactorily described by the solution of the one-dimensional heat-conduction equation. The temperature at the moment of breakdown was calculated on this basis. In so doing, the experimentally determined time from the start of the pulse to the moment of breakdown was employed. The temperature of the surface at the moment of breakdown was also measured in Ref. 80. However, in Ref. 80 the diffusion regime was realized in the vapor-gas mixture, and there was no intense vaporization of the surface. It was noted that in this case the temperature of the surface at the moment of breakdown dropped sharply with increasing intensity of the incident radiation. In Ref. 128 the breakdown temperature for conditions of this experiment was calculated on the basis of the nonstationary ionization condition (60). For the intensities considered, the maximum energy which an electron can acquire in the give field an elastic collision is higher than the ionization potential I of a metal atom, so that elastic losses are not significant. Neglecting in Eq. (41) ν_m and ν_d, we obtain the following expression for the ionization rate

$$\nu_i=\varepsilon_m\nu_m/\Delta.$$

Substituting this expression into Eq. (60) we obtain an equation for the temperature. The temperature computed in this manner, together with the experimental values[127] and thermophysical characteristics of the metals considered, are presented in Table VI.

Figure 10 displays the surface temperature of copper at breakdown versus the radiation intensity; the dots indicate the results of Ref. 127. The dashed line is the boiling point.

4.2. Heating and vaporization of microdefects

The formation of SLP associated with this mechanism was investigated in Refs. 2, 3, 19, 40–43, 49, 50, 56–59, and 129–135. The duration of the laser pulses was several microseconds, and the characteristic pulse rise times were 10–100 nsec. According to the ideas developed in Refs. 19, 40, 49, 56, 136 and other works, the first focus of SLP appears as a result of ionization of the metallic vapor, formed with the vaporization of one or another microdefect. Breakdown of pure metal vapor occurs more easily

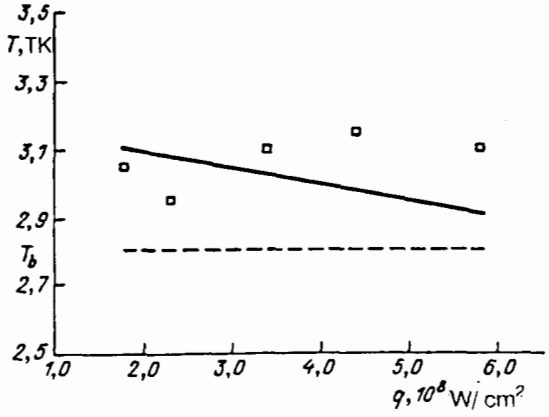

FIG. 10. Copper surface temperature at breakdown versus radiation intensity. The dots are the experimental points of Ref. 127; the curve represents the calculations of Ref. 128; the dashed line: $T=T_b$.

than breakdown of a mixture with a molecular gas. For this reason, the vapors should displace the surrounding molecular gas,[19] i.e., for a defect RDV in the hydrodynamic regime should be realized. This requires that $T^*\geqslant T_b$. The thickness of flake-type defects is determined by Eq. (13), and the size of the vapor cloud is determined by Eqs. (16) and (17). The possibility of development of an avalanche in a vapor cloud is determined by the inequality $q\geqslant q_m$, where q_m is found from Eq. (45). The region in the E-q plane where the inequalities $E\geqslant E_b$ and $q\geqslant q_m$—the region of breakdown–are satisfied is constructed in Fig. 11. The laser pulses characteristic for TEA lasers are also constructed in the same coordinates. Three plasma formation regimes are possible, depending on the position with respect to the region of breakdown (see Fig. 11):

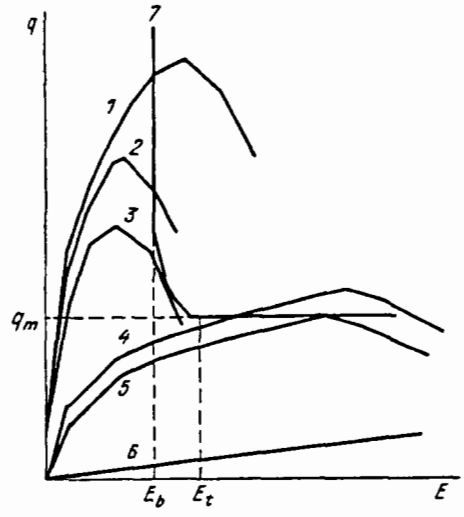

FIG. 11. Boundaries of the regions of values of E and q where plasma formation on microdefects (7) occurs; for pulses *1–3* $E=const$; for the pulse *4*—$q=$const; *3*, *5*—threshold situations, 6—(no Russian text, incomplete)

$E=const$. The laser pulse intersects the vertical branch of the boundary of the region of breakdown, plasma formation occurs when a definite value of E is reached. This regime is possible on both the leading, growing edge and on the trailing edge of the pulse (curves *1* and *2*).

$q=const$. The laser pulse intersects the horizontal branch—the boundary of the region of breakdown. This regime is possible only on the leading edge of the pulse (curve *4*).

Threshold regime. The laser pulse touches the boundary of the breakdown region. Plasma does not arise when the pulse energy is decreasing. For the pulse shape considered, the threshold regime is possible either on the trailing section of the pulse (3) or if the top of the pulse touches the boundary of the breakdown region (5).

The thresholds of SLP formation under the action of a pulsed CO_2 laser on the surface of different metals were investigated in Ref. 56. The pulse parameters were presented in Sec. 2.2. The plasma-formation time t_d (so-called delay time) was measured as a function of the total energy of the laser pulse per unit area E_τ for different metals and areas of the focusing spot of the laser beam. It was found that these experimental data could be used to calculate the values of $E(t)$ and $q(t)$ at the moment of breakdown. The results of such a calculation, performed in Ref. 61, are presented in Fig. 12. The curves are drawn through the experimental data. As one can see from the figure, for Bi, Al, and polished copper (curves *1–3*) plasma formation occurs with $q=$const, with the exception of a comparatively narrow range of low energies E_τ. Unpolished copper (curves *4*) corresponds to plasma formation with $E=$const. The breakdown values of E and q, corresponding to this experiment, were also calculated in Ref. 61. The thicknesses of the defects for Bi, Al, and polished copper were also chosen to be 0.1 μm, while for unpolished copper the defects were assumed to be 0.4 μm thick. The areas of the defects varied from $7\cdot10^{-7}$ to $4\cdot10^{-6}$ cm^2. In Fig. 11 the corridor between the computed values of E_b and E_t is hatched for each metal. One can see that for Bi, Al, and polished copper most of the experimental points correspond to $E>E_t$, i.e., breakdown occurs after the defect is vaporized. The computed values of q_m (marked by arrows in Fig. 12) agree with the experimental values of the breakdown intensity. For unpolished copper the breakdown values of E are close to E_b, and $q_m<q$.

The conditions for plasma formation on the surface of duraluminum and glasses under the action of microsecond CO_2-laser pulses were likewise investigated in Ref. 130. It was found that this happens for $E=$const.

It was assumed above that the focusing spot contains a quite large number of microdefects. In this case the effect of their statistical properties is found to be smoothed out. However, under real conditions the focusing spot contains a small number of defects with significantly different sizes. In this situation it is important to take into account their statistical properties in order to determine the plasma-formation thresholds. In the experiment this is manifested as a so-called size effect, a sharp increase of the surface energy of a laser pulse required for formation of SLP, with

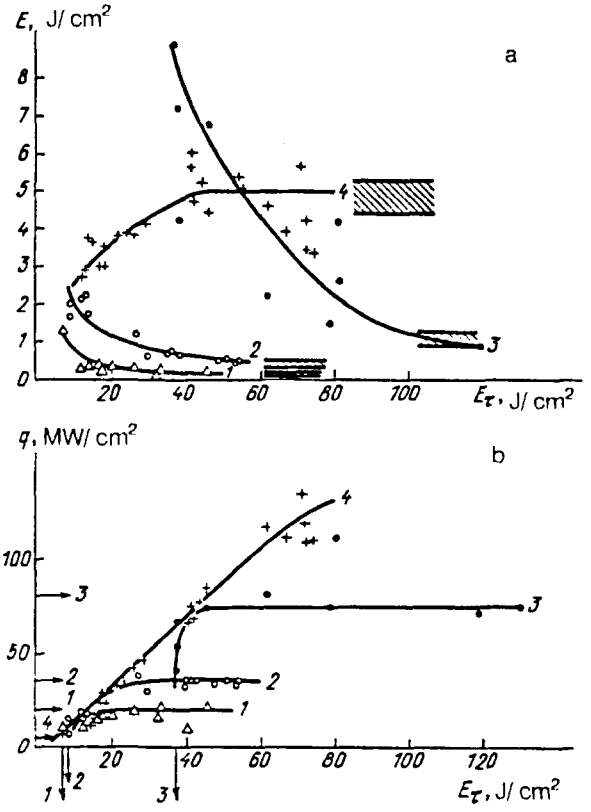

FIG. 12. Specific surface energy E of a laser pulse (a) and intensity q (b) at the moment of plasma formation versus the total surface energy E_τ in the experiment of Ref. 56. Δ, *1*—Bi; o, *2*—Al; o, *3*—polished copper; Δ, *4*—unpolished copper; regions between the computed values of E_b and E_t are hatched; the arrows mark on the abscissa the threshold values of E_τ and on the ordinate the computed values of q_m for the corresponding metals.

a decrease of the radius of the focusing spot and in the existence of some threshold spot radius for which the plasma first appears. The size effect has been observed in many works.[56,121,136,137] In Ref. 121 it was observed that as the diameter of the irradiation spot increases, the threshold of breakdown of air under the action of ~1 μsec CO_2-laser pulse with a 0.2 μsec spike at the surface of metallic and dielectric targets decreases significantly. The size dependence of the threshold for manifestation of irreversible changes in the optical characteristics as a result of breakdown at the surface of a number of transparent dielectrics and metallic mirrors was investigated under close conditions in Ref. 136.

We now consider, following Ref. 135, the effect of the size and number spread of defects within the focusing spot on the plasma-formation threshold for the experimental conditions of Ref. 56.

Let a surface microdefect in the form of a flake of thickness d and area S be present on the surface. The focusing spot can contain N defects with different thicknesses d and areas S. Only defects for which

$$\Sigma(d)\leqslant E,\quad q_m(d,S)\leqslant q \tag{63}$$

can initiate plasma. We note that, as a rule, the difference between E^* and E_t (see Eqs. (11) and (14)) is not great. In order to simplify somewhat the breakdown criterion we can choose for Σ in Eq. (63) $E^* \approx E_b$ or $(E^*+E_t)/2$. The inequalities (63) bound the thickness of the defect and its minimum possible volume. It is convenient to express the thickness and area of defects in relative units $d'=d/\langle d\rangle$ and $S'=S/\langle S\rangle$, where $\langle d\rangle$ and $\langle S\rangle$ are average values. For the energy density E and intensity q we introduce the dimensionless units $E'=E/\Sigma(d)$ and $q'=q/q_m(d,S)$. In what follows the primes on the dimensionless variables will be dropped. Then the inequalities (63) will have the form

$$d \leqslant E, \quad S \geqslant 1/q^{3/2}d. \tag{64}$$

We define by the following expression the probability of finding a defect satisfying these inequalities:

$$P(d<E, \quad S>1/q^{3/2}d) = \int_0^E \mathrm{d}\, d f(d) \int_{1/q^{3/2}}^{S'} \mathrm{d}S f(S), \tag{65}$$

where $f(d)$ and $f(S)$ are the thickness and area probability distributions of the defects. The integral over S in Eq. (65) is bounded by some maximum value $S' \sim 1/\langle S\rangle n_d$, where n_d is the average concentration of surface defects. If the average number of defects in a spot with radius R is $N=\pi R^2 n_d$, then for defects leading to the formation of plasma for fixed E and q the average concentration is

$$N_p = NP = \pi R^2 n_d P. \tag{66}$$

In order for a plasma to appear there must be not less than one such defect within the focusing spot. Assuming that the fluctuations of the number of defects within an area of πR^2 are described by a Poisson distribution, we find that the probability that the size of a defect satisfies the breakdown conditions (15) and the number of such defects within the focusing spot is not less than unity is

$$W = (d \leqslant E, \quad S \geqslant 1/q^{3/2}d, \quad N_p \geqslant 1) = 1 - \exp(-PN). \tag{67}$$

The quantity W plays the role of the probability of plasma formation with prescribed parameters of the laser pulse E and q. It follows from Eq. (67) that if $PN>1$, this probability is close to unity. Thus when there is a distribution of defects over size and number within the focusing area, we can talk about plasma formation only with a certain probability W. We choose some value of W quite close to 1. Then

$$P = (1/N)\ln[1/(1-W)] = 1/N^*, \tag{68}$$

where $N^* = N/\ln[1/(1-W)]$ is the effective number of defects within the area of the focusing spot. This is equivalent to introducing an effective concentration of defects $n_d^* = n_d/\ln[1/(1-W)]$. For $W=0.63$ we have $N=N^*$, and for $W=0.864$ we have $N^*=N/2$. Solving Eq. (68) for E and q with known distributions of defects over size and area $f(d)$ and $f(S)$, respectively, we find in the E-q plane the dependence of the boundary of the breakdown region on the effective number N^* of defects. Calculations of this type were performed in Ref. 135. Here, there naturally arises the question of the form of the distributions f. We do not know of any experimental data on this question. The distribution can be chosen on the basis of the criterion of unique saturation of the size effect—the boundary of the breakdown region must be independent of N for sufficiently large values of N. For positive-definite random quantities d and S this requirement is satisfied by the log-uniform or log-normal probability distribution. These distributions were used to calculate the position of the boundary of the breakdown region for the experimental conditions of Ref. 56. Figure 13 displays the boundaries of the breakdown region and the position of the pulse for unpolished (a) and polished (b) copper. It is obvious that there is a qualitative difference between these cases. For unpolished surfaces the top of the pulse is always located to the left of the breakdown region and plasma formation in the threshold and nonthreshold regimes occurs on the trailing edge of the pulse. For polished surfaces the top of the pulse lies to the right of the breakdown region, and for this reason threshold regimes are realized when the top of the pulse touches the horizontal branch of the breakdown region or the pulse passes through the breakpoint at the onset of the descending section of the laser pulse. It is also important that for unpolished surfaces the regime $E=$const is realized when E_τ exceeds some threshold values (curves *3* and *4* in Fig. 13a), while for a polished surface $q=$const (curves *3* and *4* in Fig. 13b).

In Fig. 14 the total pulse energies E_τ are plotted as functions of the area S_p of the focusing spot for unpolished and polished surfaces (curves *1* and *2*, respectively). The calculations agree with the experimental data.

4.3. Heating and vaporization of aerosols

The first experimental investigations of breakdown of gases by laser radiation were performed for small focal volumes $\sim 10^{-3}$ cm^3. The concentration of aerosol particles in laboratory air does not exceed 10^2 cm^{-3}. It is obvious that under such conditions the effect of aerosol on the breakdown threshold of air could not be observed. The role of aerosol particles in reducing the threshold for optical breakdown of gases was observed by switching to experiments with large focal volumes and observing the anomalous dependence of the breakdown threshold of contaminated air as a function of the size of the focusing spot. Thus in Ref. 9 the intensity of breakdown was investigated, for both pure air and air with aerosol particles, as a function of the diameter of the focal spot. In the latter case the breakdown threshold dropped appreciably with increasing size of the focal spot. This was observed for focal spot sizes when diffusion losses of electrons should have no effect. This fact indirectly indicates that the threshold for particle-initiated optical breakdown depends on the particle size.

A common feature of all models describing breakdown in dispersed aerosol media is the assumption that the aerosol particles are heated by the laser radiation. Most models consider aerosol particles as a factor facilitating breakdown due to the development of an electron avalanche in the products of breakup of the particles. The model of an elec-

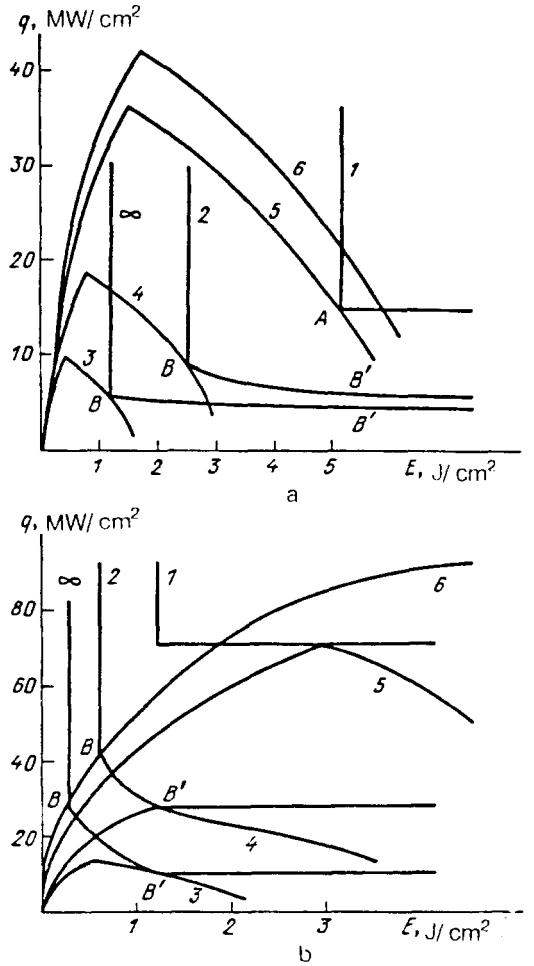

FIG. 13. Boundaries of the breakdown region for unpolished (a) and polished (b) copper with $N^*=1$ (*1*), 2 (*2*), ∞ (∞). The pulses *3–5* correspond to threshold conditions; the pulse *6*, a corresponds to $E=$const and the pulse *6*, b corresponds to $q=$const.

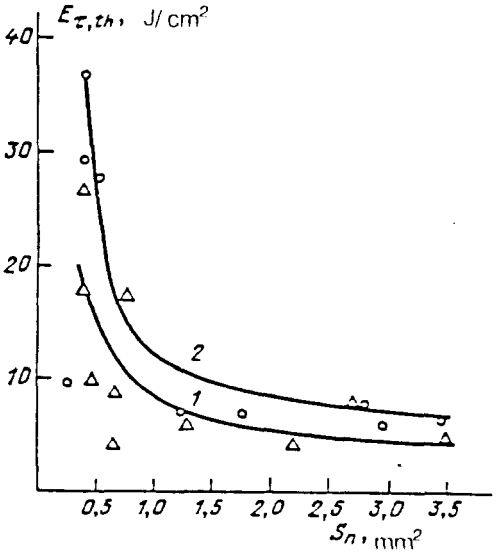

FIG. 14. Experimental[56] (points) and computed (curves) values of E_τ versus the area of the focusing spot for unpolished (*1*, triangles) and polished (*2*, circles) copper.

tron avalanche was consistent with the first experimental results on breakdown in the presence of aerosol particles.[9,10] In particular, it is consistent with the fact that the breakdown threshold for 1.06 μm radiation is approximately 100 times higher than for 10.6 μm radiation. This frequency dependence of the threshold intensity of breakdown is characteristic for the electron-avalanche mechanism. Two approaches are used to describe this dependence. The first approach is known as a "thermal explosion"[9,67] and it starts from the assumption that the particles explode under the action of the laser radiation. In the second—vaporization—approach it is assumed that a particle is heated, its vapors expand hydrodynamically, and a cloud is formed.[67] In both cases breakdown occurs due to development of an electron avalanche in the products of breakup of the particle. According to the thermal-explosion model the particle absorbs energy $W=\sigma qt$ from the laser. If the time t does not exceed the time of inertial confinement of the particle R/v_s (v_s is the sound speed in the solid body) and the absorbed energy is sufficient for complete vaporization of the particle $W\geqslant 4\pi R^3\rho\Lambda/3$, then the vaporization process acquires the character of an explosion. The threshold intensity required for explosion of the particle is

$$q_{\text{exp}}=4\rho\Lambda v_s/3\zeta,$$

where $\zeta=\sigma/\pi R^2$.

As the vapor expands, the density of atoms in the vapor drops from the density of the solid body $\sim 5\cdot 10^{22}$ cm^{-3} to the density of the surrounding medium (air), and in the process it passes through a value for which the rate at which electrons acquire energy due to the inverse bremmstrahlung in the field of the wave is maximum.

The maximum value of $d\varepsilon/dt$ is realized for $\omega=\nu_m$. The optimal concentration of atoms for energy acquisition is $\sim 10^{20}$–10^{22} cm^{-3}. For $\omega=\nu$ the threshold intensity for avalanche development, taking into account diffusion losses, has the form[67]

$$q_0=cI^2[1+(\zeta v_s\omega^2/3v_e^2)]/2e^2R^2.$$

The maximum reduction of the threshold intensity for breakdown in the process of avalanche development in the vapors of the particle can reach a factor 50 compared to the case of avalanche development in air.[9] The threshold intensity must equal the larger of the two quantities q_{exp} and q_0. The intensity of a thermal explosion of a particle is limited from above by the intensity of the breakdown of pure air.

As already mentioned, many authors started from the assumption that there is no explosion and a particle vaporizes slowly. In particular, in Refs. 68 and 69 the estimates made according to the explosion model gave breakdown threshold intensities higher than the experimentally observed values. These works investigated breakdown of argon, containing Al_2O_3 powder, by 30–100 nsec neodymium laser pulses with intensity 10^8–10^{13} W/cm^2. Spectra of the plasma forming on breakdown and containing both lines of

the particle matter (Al, Al_2O_3) at low pressures ($p \sim 0.5$ torr) and lines of the filler gas (Ar) at pressures of the order of 1 atm were measured. The attenuation coefficient of the heterogeneous medium was measured. Above a threshold intensity ($q \sim 10^8$ W/cm^2) the values of the attenuation coefficient increase rapidly. The intensity at which the aerosol particles are completely vaporized was estimated to be $1.5 \cdot 10^8$ W/cm^2. The characteristic plasma development time was 70–80 nsec. Over this time the matter of the particles vaporizes, breakdown develops in the vapors, and the argon atoms are excited by free electrons. On the basis of the experimental results it can be stated that a laser-produced spark can form in dense heterogeneous media even without explosion of the particles, and this results in lower breakdown thresholds.

Besides the models based on the theory of cascade avalanche ionization, there also exist models in which the formation of a vapor layer around a particle is considered as an intermediate stage facilitating ionization of the air. Thus in Ref. 138 it was suggested that expansion of the vapors of the particle engenders in the surrounding medium a shock wave in which the air is heated and ionized. The maximum temperature up to which the air can be heated in the shock wave was estimated as a function of the optical thickness of the particle (KR, where K is the absorption coefficient of the particle) for a number of values of the intensity of the laser radiation. It is suggested that heating of the air up to a temperature $T \sim 0.1I$ creates conditions for initiation of an optical discharge in it. Curves of the threshold breakdown intensity versus the aerosol particle radius were constructed.

In Ref. 139 a thermal mechanism of breakdown of air containing suspended glass filaments was proposed. A discharge on 1-100 μm in diameter glass filaments was investigated with the help of 1-30 μsec CO_2-laser pulses with intensity of 10^6–10^7 W/cm^2. It was found that the breakdown threshold intensity decreases significantly and the plasma formation time increases with increasing size of the laser focal spot. The authors explain this effect by the fact that as the size of the focal spot increases, the vapors formed as the filament is heated reside for a longer time in the laser beam and are heated up to the breakdown temperature at a radiation intensity lower than in the case of a small focal spot. The breakdown development time then increases. The threshold temperature for appearance of a discharge is taken to be the temperature at which the absorption of radiation by electrons due to the inverse bremmstrahlung produces a highly ionized plasma very rapidly. The experiments of Ref. 130 showed that the breakdown intensity is a weak function of the filament diameter D ($q \sim 1/D^{1/3}$).

The original mechanism of breakdown of aerosols due to "hopping" electrons was proposed in Ref. 140. The crux of this mechanism is as follows. Any electron whose kinetic energy at the boundary of the particle exceeds the work function A_0 of the particle material escapes from the surface of the particle. The retarding Coulomb field of the charged particle acts on the electron. The thermionic emission flux from the particle consists of electrons whose energy exceeds the effective work function A, which equals the work function A_0 and the energy required in order to overcome the retarding Coulomb field. Electrons with energies in the range $A_0 < \varepsilon < A$ return to the particle eventually after escaping from it. For this reason they can be termed "hopping" electrons. Each hopping electron extracts from the electromagnetic field and gives up to the particle some energy which is expended on heating the particle. If the hopping electron collides with a molecule of the gas surrounding the particle, the energy of the electron goes into ionizing the surrounding gas. In this manner both channels for conversion of the energy of the incident radiation lead to development of an optical discharge (the first channel by the particle thermal explosion mechanism and the second by the traditional avalanche ionization mechanism, in which the charged particle plays the role of the main scatterer).

The model of self-focusing of laser radiation occupies a special place among models of breakdown of aerosols.[140] This model was proposed in order to explain the experimental results obtained in Ref. 140. The breakdown threshold intensity of air at 1.06 μm was investigated as a function of the geometry of the focal volume. It was shown that as the length of the caustic increases, the breakdown threshold decreases significantly. At the same time, as the focal volume increases with constant length of the caustic, the breakdown threshold remains virtually unchanged. These results contradict the thermal-explosion theory and the vaporization model of breakdown of aerosols, according to which the breakdown threshold must depend strongly on the focal volume. According to the self-focusing model, aerosol particles suspended in air are vaporized by the laser radiation, and initial electrons with concentration $n_e \sim 10^{14}$ cm^{-3} are thereby produced by means of thermionic emission. The free electrons, being accelerated in the field of the light wave, excite the air molecules, but the energy of the molecules is too low for ionization of the molecules. The presence of excited molecules increases the index of refraction of the medium, and this gives rise to self-focusing of the laser radiation, resulting in breakdown of the air. An important feature of this model is that the threshold does not depend on the size of the aerosol particles. A similar result was obtained in Ref. 143, where the breakdown threshold was determined according to the appearance of appreciable attenuation of CO_2-laser radiation passing through the aerosol. It was found that the thresholds for blocking the laser radiation were close for different aerosols, differing by the size and material of the aerosol particles.

In spite of the existence of a large number of models and diverse approaches for describing breakdown in dispersed aerosol media, even here the "vaporization model" based on the thermal and ionization conditions has a quite wide range of application. We now discuss this model in somewhat greater detail, following Ref. 66.

The criterion for breakdown of a separate aerosol particle in the hydrodynamic regime has the form

$$E > E_b > E^*, \quad q^* > q > q_R, \tag{69}$$

where q_R is determined by Eq. (45), if R is calculated according to Eq. (31). The point of the inequalities (46) is that a particle is in the RDV and its vapors displace the surrounding gas. In the aerosol the particles have a size distribution. This distribution is usually described by Jung's formula[67]

$$f(r)=(\beta-1)(r/r_m)^{\beta}/r_m \quad (r\geqslant r_m), \tag{70}$$

where r_m is the minimum particle radius. For carbon particles, for example, $\beta=5$ and $r_m=0.1$ μm. It is convenient to switch to the dimensionless particle radius $r'=r/r_m$. We also introduce the dimensionless energy $E'=E/E''_*$ and dimensionless intensity $q'=q/q''_v$, where $E''_*=4\rho cT^*r_m/3\zeta$ and $q''_v=\pi^2\Delta l^2/3\varepsilon'_\omega(\rho/\rho_v)^{2/3}r_m^2$. The latter intensity corresponds to development of ionization in the vapor cloud when a particle of minimum size is vaporized. Using these variables we obtain from Eqs. (69) and (45) the following expression, for the case $r>r_c$, relating the test quantities E', q'', and r' (the primes will be dropped below):

$$E/r=1+3\xi[1-\{1-[1/(qr^2)^{3/2}]\}]^{1/3}, \tag{71}$$

where $\xi=\Lambda/cT^*$. If by the time T^* is reached the particle still has not been completely heated and the inequality $\chi t^*/r^2\ll 1$ is satisfied, then the expression (71) can be used for the heating. It can be shown that this changes somewhat the form of the expression (71).

The expressions obtained above are valid for an aerosol particle of fixed size. When there is some distribution of particle sizes the concept of maximum particle size r_M is usually introduced. It is related to the distribution function by the following relation:

$$\int_{r_M}^{\infty} f(r)\mathrm{d}r=(NV)^{-1}.$$

Using the distribution (70) we obtain

$$r_M=r_m(NV)^{1/(\beta-1)};$$

where V is the focal volume.

For known laser parameters E and q the breakdown condition can be written in the form of an inequality for r. Thus in the case of complete vaporization of a particle breakdown will occur if $qr^2\geqslant 1$ (here dimensionless units are employed) or

$$r\geqslant 1/q^2V$$

In the case of incomplete vaporization, when Eq. (31) holds, the analogous inequality has the form[60]

$$r\geqslant F=1/[q^{1/2}\{1-[(E-E^*)^3/\zeta]\}^{1/3}]. \tag{72}$$

The probability of finding a particle satisfying the condition (72) is obtained from here using Eq. (70):

$$P(r\geqslant F)=F^{1-\beta}. \tag{73}$$

Breakdown requires that the focal volume contain at least one particle satisfying the inequality (72). Using Poisson's distribution, as done for microdefects, we obtain

$$r_M/w^{1/(\beta-1)}=F, \tag{74}$$

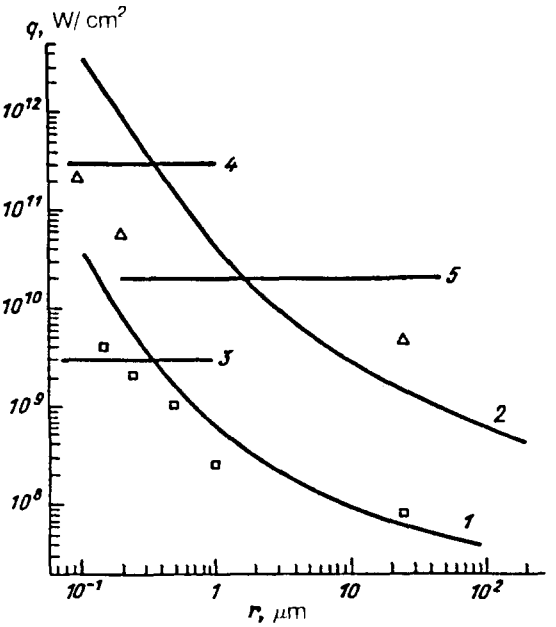

FIG. 15. Experimental breakdown threshold intensities for a as a function of the radius of carbon aerosol particles suspended in air in the experiments of Ref. 9 (CO_2 laser) (light colored points) and Ref. 10 (Nd laser) (dark points), the theoretical curves for Ref. 9 (*1*) and Ref. 10 (*2*) and the breakdown levels for pure air for Ref. 9 (*3*) and Ref. 10 (*4*), as well as the calculations according to the explosive model of Ref. 67 (*5*).

where $w=-\ln(1-W)$. Comparing Eq. (74) to Eq. (72), we can see that taking into account the spread of the particles over particle radii reduces to replacing the fixed particle radius r by an effective quantity $r_M/w^{1/(\beta-1)}$. For carbon $\beta-1\approx 4$, so that $w^{1/(\beta-1)}\approx 1$. This makes it possible to find the breakdown intensity and energy as a function of the maximum particle size. The latter quantity is related to N and V.

In his experiments, which are now classics, D. Lencioni[9,10] investigated breakdown intensities as a function of the maximum size of carbon aerosol particles in air and as a function of the size of the focusing spot for 200 nsec CO_2-laser pulses and 50 nsec Nd-laser pulses. The intensity varied from 10^8 up to 10^{10} W/cm^2. Small particles ($r\leqslant 1$ μm) were introduced in the form of a finely dispersed mixture into the focal volume. In addition, measurements were performed for a single large 25-μm carbon particle, introduced into the focal volume. The experimental data are displayed in Fig. 15. The breakdown intensities for the smallest particles correspond to the values for breakdown of pure air (lines 3 and 4 in Fig. 15). As the maximum particle radius increases, the breakdown intensities drop significantly. In Fig. 15 the curves *1* and *2* were constructed according to the model described above, taking into account the statistics of small aerosol particles. These curves reflect qualitatively correctly the experimental relations. For small particles, especially in the case of the Nd laser, the computed values are somewhat higher than the experimental values. This could be connected, on the one hand, to inadequate information about the aerosol particles, their aggregate state, the presence of impurities, po-

rosity, and so on, and on the other to the limitations of the model itself.

In Fig. 15 the intensity according to the explosive model[67] is marked by a horizontal line (the intensity does not depend on the laser wavelength and the particle size). As one can see, it lies above the experimental points obtained in the experiments with the CO_2 laser. For the Nd laser the breakdown intensities for 0.1 μm particles are identical to the values for pure air. For 0.2 μm particles the breakdown intensity lies below the computed values, but above the predictions of the explosive model. It is possible that some intermediate case is realized here.

It is of interest to determine the condition under which the vapor clouds from separate particles, vaporizing in the hydrodynamic regime, merge. This condition is important for determining the threshold characteristics of collective optical breakdown, studied in Sec. 3.2, in an aerosol medium.[92] Let $r > r_c$ and let the volume of the vapor cloud from a separate particle be determined by the expression (45). We introduce the random function

$$V_N = \frac{4\pi}{3} \sum_{i=1}^{N} R_i^3$$

which is the total volume of vapor from all N aerosol particles in the focal volume V. The random quantities R_i^3 have the same average values $\langle R_i^3 \rangle$ and variance $D^2 = \langle (R^3 - \langle R^3 \rangle)^2 \rangle$. For example,

$$\langle R^3 \rangle = \int_{r_m}^{\infty} f(r) \mathrm{d}R^3(r).$$

Using the distribution (70) and calculating the integral, we obtain

$$\langle R^3 \rangle = 4_m^3 (\rho/\rho_v) \{1 - [1 - (3\xi/4)]/E\}.$$

The condition that the vapor clouds overlap can be written in the form

$$V_N \geqslant \eta V, \tag{75}$$

where the coefficient η is of order unity, and corresponds, for example, to close-packing of spheres. The inequality (75) can be rewritten in the form

$$\frac{1}{N} \sum_{i=1}^{N} R^3(r_i) > 3\eta/4\pi n, \tag{76}$$

where $n = N/V$ is the concentration of aerosol particles in the focal volume. The left-hand side of the inequality (76) is the average (over the focal region) volume of the vapor cloud created by a separate particle. If the number N is sufficiently large, then on the basis of the law of large numbers it can be assumed, to a good approximation, that

$$\frac{1}{N} \sum_{i=1}^{N} R_i^3 = \langle R^3 \rangle. \tag{77}$$

Using Eqs. (75)–(77), the overlap condition can be rewritten as an inequality on E. In dimensionless units this inequality has the form

$$E \geqslant [1 + (3\xi/4)]/[1 - (3\eta\rho_v/16\pi n r_m^3 \rho)]. \tag{78}$$

The formula (78) is valid if

$$3\eta\rho_v/16\pi n r_m^3 \rho \leqslant 1.$$

In the opposite case overlapping does not occur for any values of E. Assuming that in Eq. (78) $3\xi/4 \ll 1$ and $3\eta\rho_v/16\pi n r_m^3 \rho \ll 1$, and switching to dimensionless variables, we obtain

$$E = (\rho \Lambda r_m/\xi) + (3\Lambda m p_\infty \eta/0.67 k T_b \cdot 16\pi n r_m^2 \xi)$$

where k is Boltzman's constant and m is the mass of a vapor atom. The second term of this formula is equal, to within a numerical factor, to the term proposed in Ref. 106. The criterion (78) is the most general criterion. Under Lencioni's experimental conditions[9,10] $n = 6 \cdot 10^5$ cm^{-3} and for $r_m = 0.1$ μm overlapping cannot occur. Overlapping would have occurred if the particles were distributed according to Eq. (70) with $r_m = 1$ μm. The criterion (78) is necessary for collective optical breakdown in an aerosol medium. It must be supplemented by a sufficient condition, associated with the possibility of ionization development in vapor formed from overlapping vapor clouds from separate partially or completely vaporized aerosol particles.

5. CONCLUSIONS

The above analysis, which is based on the thermal and ionization conditions, of the appearance of SLP has in many ways made it possible to determine correctly the threshold characteristics of a laser pulse leading to breakdown. Different materials in an atmosphere consisting of atomic and molecular gases were considered. Plasma was initiated by heating and vaporization of the surface as a whole, thermally insulated microscopic irregularities of the surface, and aerosol particles. The intensities ranged from 10^5 up to 10^{11} W/cm^2. The laser pulse durations ranged from milliseconds up to several nanoseconds. Attention was focused on the primary mechanisms of plasma formation. Naturally, many important phenomena accompanying the formation of SLP could not be adequately described within the framework of the present review, and we confined our attention only briefly mentioning them (a more detailed description can be found in the cited literature). We now briefly discuss the questions meriting further investigation.

A surface laser plasma initiated by heating and vaporization of surfaces in the absence of developed vaporization of the surfaces[23] is in some sense the simplest case of an optical discharge near a surface. The kinetics of breakdown in vapor-gas mixtures, especially in atomic mixtures, has been investigated in detail.[89–100] The state of affairs is somewhat worse in the case of molecular mixtures.

Vaporization of aerosol particles, when their temperature does not exceed the boiling point, is characteristic for LCOB.[104–110] Here the vapors of the vaporized aerosol diffuse into the surrounding gas. The moment that the vapors from separate particles merge and the description of the development of ionization in the vapor-gas macrocloud formed are important. On a theoretical level, this problem has not been adequately solved, though such attempts have

been made.[108–110] In order to compare theory to experiment it is necessary to fix, for a prescribed shape of the laser pulse, the moment at which the plasma appears (delay time) with respect to the moment at which the action of the pulse starts. The procedure for performing such measurements has been developed in application to millisecond[23] and microsecond[56] pulses irradiating a surface; these are the cases discussed above.

The basic features of the mechanism of the discharge in vapors have been determined in hydrodynamic regimes, in the presence of an erosion flame, when an SLP forms due to heating and vaporization of the surface under the action of relatively long laser pulses.[26,123–125] A generally accepted mechanism for the transition from a discharge in vapor to a discharge in the surrounding gas does not exist, though interesting suggestions concerning this question have been made (see, for example, Refs. 49 and 143–149).

In the case of a target irradiated with microsecond and shorter laser pulses, attention was focused mainly on thermally insulated microdefects. Other suggestions concerning the primary microfoci have also been made in the literature.[150–155]

In the present review we have proposed a systematization and description of states of SLP (we note that similar proposals concerning classification of this object were made in Ref. 26). We hope that, in spite of the unavoidable ambiguity in a work of this kind and the possible subjectivism, the reader now has an idea of the modern research on the main mechanisms and physics of the appearance of SLP.

[1] A. N. Pirri, R. Schlier, and D. Northam, Appl. Phys. Lett. **21**, 79 (1972).
[2] A. I. Barchukov, F. V. Bunkin, V. I. Konov, and A. M. Prokhorov, Pis'ma Zh. Eksp. Teor. Fiz. **17**, 413 (1973) [JETP Lett. **17**, 294 (1973)].
[3] A. I. Barchukov, F. V. Bunkin, V. I. Konov, and A. A. Lyubin, Zh. Eksp. Teor. Fiz. **66**, 965 (1974) [Sov. Phys. JETP **39**, 469 (1974)].
[4] P. S. P. Wei, R. B. Hall, and W. E. Maher, J. Chem. Phys. **59**, 3692 (1973).
[5] W. E. Maher, R. B. Hall, and R. R. Jonson, J. Appl. Phys. **45**, 2138 (1974).
[6] A. A. Bakeev, L. A. Vasil'ev, L. I. Nikolashina, N. V. Prokopenko, A. S. Churilov, and V. I. Yakovlev, Kvant. Elektron. **2**, 1278 (1975) [Sov. J. Quantum Electron. **5**, 693 (1975)].
[7] A. M. Bonch-Bruevich, L. N. Kaporskii, and A. A. Romanenkov, Zh. Tekh. Fiz. **43**, 1746 (1973) [Sov. Phys. Tech. Phys. **18**, 1099 (1974)].
[8] R. J. Hull, D. E. Lencioni, and L. C. Marquet, *Laser Interations and Relativistic Plasma Phenomena*, New York, 1972, Vol. 2, p. 147.
[9] D. E. Lencioni, Appl. Phys. Lett. **23**, 12 (1973).
[10] D. E. Lencioni, Appl. Phys. Lett. **25**, 15 (1974).
[11] A. A. Uglov and M. M. Nizametdinov, Fiz. Khim. Obrob. Materialov **2**, 133 (1977).
[12] A. L. Galiev, L. A. Krapivin, L. I. Mirkin, and A. A. Uglov, Dokl. Akad. Nauk SSSR **251**, 336 (1980) [Sov. Phys. Dokl. **25**, 208 (1980)].
[13] A. A. Vedenov and G. G. Gladush, *Physical Processes During Laser Working of Materials* [in Russian], Energoatomizdat, Moscow, 1985.
[14] A. Kantrovitz, Astronaut. Aeronautics **10**, 74 (1972).
[15] F. V. Bunkin and A. M. Prokhorov, Usp. Fiz. Nauk **119**, 425 (1976) [Sov. Phys. Usp. **19**, 561 (1976)].
[16] J. T. Kare in Proceedings of the 17th International Symposium on Shock Waves and Shock Tubes, Bethlehem, 1989, p. 359.
[17] J. F. Ready, *Effects of High-Power Laser Radiation*, Academic Press, N.Y., 1971.
[18] S. I. Anisimov, Ya. I. Imas, G. S. Romanov, and Yu. V. Khodyko, *Action of High-Power Radiation on Metals* [in Russian], Nauka, Moscow, 1970.
[19] V. P. Ageev, S. G. Burdin, I. N. Goncharov, V. I. Konov, I. M. Minaev, and N. I. Chapliev, "Interaction of high-power laser pulse with solids in gases," Itogi nauki tekhniki. Ser. Radiotekhnika. M. Zh VINITI 31, 3 (1973).
[20] G. M. Weyl, *Laser-Induced Plasmas and Application*, edited by J. L. Radziemski, Marcel Dekker, 1989.
[21] V. I. Manzhukin, A. A. Uglov, and B. N. Chetverushkin, Kvant. Elektron. **10**, 679 (1983) [Sov. J. Quantum Electron. **13**, 419 (1983).
[22] V. A. Danilychev and V. D. Zvorykin, Tr. FIAN **142**, 117 (1983).
[23] E. V. Dan'shchikov, V. A. Dymshakov, F. V. Lebedev, and A. V. Ryazanov, Kvant. Elektron. **12**, 1863 (1985) [Sov. J. Quantum Electron.
[24] F. V. Bunkin and M. I. Tribel'skii, Usp. Fiz. Nauk **130**, 193 (1980) [Sov. Phys. Usp. **23**, 105 (1980)].
[25] V. B. Fedorov, Tr. FIAN **10**, 75 (1988).
[26] A. M. Bonch-Bruevich, I. A. Didenko, and L. N. Kaporskii, "Low-threshold optical breakdown of gases near a surface," Preprint No. 13, Institute of Heat and Mass Transfer, Academy of Sciences of the Belorussian SSR, Minsk, 1985.
[27] R. V. Arutyunyan, V. Yu. Baranov, L. A. Bol'shov, D. D. Malyuta, and A. Yu. Serbant, *Action of Laser Radiation on Materials* [in Russian], Nauka, Moscow, 1989.
[28] M. F. Kanevskii, A. Yu. Serbant, and S. Yu. Chernov, *Review of Dynamics of Surface Low-Temperature Laser Plasma* [in Russian], Institute of Atomic Energy, Moscow, 1990.
[29] W. Duley, *Laser Processing and Analysis of Materials*, Plenum Press, N.Y., 1983.
[30] H. Hora, Physics of Laser-Driven Plasmas, Wiley, N.Y., 1981.
[31] Yu. V. Afanas'ev, R. G. Basov, O. N. Krokhin *et al.*, *Interaction of High-Power Laser Radiation with Plasma* [in Russian], VINITI, Moscow, 1978.
[32] S. Atzeni, "The physical basis for numerical fluids simulations in laser fusion," Plasma Phys. Contr. Fusion 29, 1535 (1987).
[33] J. Dudershtadt and H. Moses, *Inertial-Confinement Thermonuclear Fusion* [Russian translation], Energoatomizdat, Moscow, 1984.
[34] S. Eliezer, A. Ghatak, and H. Hora, *An Introduction to Equation of State: Theory and Applications*, Cambridge University Press, Cambridge, 1986.
[35] G. G. Vilenskaya and I. V. Nemchinov, Zh. Prikl. Mekh. Tekh. Fiz., No. 6, 3 (1969).
[36] G. G. Vilenskaya and I. V. Nemchinov, Dokl. Akad. Nauk SSSR **186**, 1048 (1969) [Sov. Phys. Dokl. **14**, 560 (1969)].
[37] Yu. V. Afanas'ev and O. N. Krokhin, Tr. FIAN **52**, 118 (1970).
[38] C. Knight, AIAA J. **17**, 519 (1979).
[39] V. I. Igoshin and V. I. Kurochkin, Kvant. Elektron. **11**, 1556 (1984) (*sic*).
[40] G. M. Weyl, A. N. Pirri, and R. Root, AIAA J. **19**, 460 (1981).
[41] A. V. Bessarab, N. V. Zhidkov, and S. B. Kormer, Kvant. Elektron. **5**, 325 (1978) [Sov. J. Quantum Electron. **8**, 188 (1978)].
[42] C. T. Walters, R. H. Barnes, and R. E. Beverly III, J. Appl. Phys. **49**, 2937 (1978).
[43] A. V. Bessarab, V. M. Romanov, and V. N. Samylin, Zh. Tekh. Fiz. **48**, 1751 (1978) [Sov. Phys. Tech. Phys. **23**, 995 (1978)].
[44] V. E. Zuev, Yu. D. Kopyshin, and A. V. Kuzovskii, *Nonlinear Optical Effects in Aerosols* [in Russian], Nauka, Novosibirsk, 1980.
[45] V. E. Zuev, A. A. Zemlyanov, Yu. D. Kopyshin, and A. V. Kuzikovskii, *High Power Laser Radiation in an Atmospheric Aerosol* [in Russian], Nauka, Novosibirsk, 1984.
[46] Yu. D. Kopytin, Yu. M. Sorokin, A. M. Skripkin, and N. N. Belov, *Optical Discharges in Aerosols* [in Russian], Nauka, Novosibirsk, 1990.
[47] Yu. V. Arkhipov, I. N. Belashkov *et al.*, Kvant. Elektron. **13**, 103 (1986) [Sov. J. Quantum Elektron. **16**, 63 (1986)].
[48] V. I. Kolachev, E. A. Livanov, and V. I. Elagin, *Metal Science and Heat Treatment of Metals and Alloys* [in Russian], Metallurgiya, Moscow, 1981.
[49] V. I. Konov, Izv. Akad. Nauk SSSR, Ser. Fiz. **46**, 1044 (1982).
[50] N. D. Ustinov, V. N. Moiseev, V. A. Tikhomirov, I. R. Troitskii, and M. M. Shugaev, Kvant. Elektron. **13**, 918 (1986) [Sov. J. Quantum Electron. **16**, 601 (1986)].
[51] Yu. K. Danileiko, A. A. Manenkov, A. M. Prokhorov, Ts. Ts. Khaimov, and V. Ya. Mal'tsev, Zh. Eksp. Teor. Fiz. **62**, 100 (1972) [Sov. Phys. JETP **35**, 54 (1972)].

[52] I. V. Alishin, A. M. Bonch-Bruevich, V. I. Zinchenko, Ya. I. Imas, and V. L. Komolov, Zh. Tekh. Fiz. **43**, 2625 (1973) [Sov. Phys. Tech. Phys. **18**, 1648 (1974)].
[53] N. Bloembergen, Appl. Opt. **12**, 661 (1973).
[54] V. P. Ageev, S. G. Burdin, V. I. Konov, S. A. Uglov, and N. I. Chapliev, Kvant. Elektron. **10**, 780 (1983) [Sov. J. Quantum Electron. **13**, 483 (1983)].
[55] A. E. Negin, Kvant. Elektron. **14**, 1450 (1987) [Sov. J. Quantum Electron. **17**, 923 (1987)].
[56] I. Ursu, I. Apostol, M. Dinescu, A. Heinig *et al.*, J. Appl. Phys. **58**, 1765 (1985).
[57] E. A. Bernichenko, A. V. Koshkin, A. P. Sobolev, and B. T. Fedyushin, Kvant. Elektron. **11**, 842 (1984) [Sov. J. Quantum Electron. **14**, 570 (1984)].
[58] E. A. Bernichenko, A. V. Koshkin, A. P. Sobolev, and B. T. Fedyushin, Kvant. Elektron. **8**, 1582 (1981) [Sov. J. Quantum Electron. **11**, 953 (1981)].
[59] V. A. Danilychev, V. D. Zvorykin, I. V. Kholin, and A. Yu. Chugunov, Kvant. Elektron. **7**, 2599 (1980) [Sov. J. Quantum Electron. **10**, 1518 (1980)].
[60] M. Born and E. Wolf, *Principles of Optics*, Pergamon Press, N.Y., 1969.
[61] V. S. Vorob'ev and S. V. Maksimenko, Kvant. Elektron. **15**, 2537 (1988) [Sov. J. Quantum Electron. **18**, 1595 (1988)].
[62] N. N. Belov, Kolloid. Zh. **5**, 987 (1987).
[63] J. P. Barton and D. R. Alexander, J. Appl. Phys. **79**, 7973 (1991).
[64] N. N. Belov, Opt. Spektrosk. **61**, 1331 (1986).
[65] D. C. Smith, J. Appl. Phys. **48**, 2217 (1977).
[66] I. Yu. Borets-Pervak and V. S. Vorob'ev, Kvant. Elektron. **20**, 264 (1993) [Sov. J. Quantum Electron. **23**, 224 (1993)].
[67] F. V. Bunkin and V. V. Savranskii, Zh. Eksp. Teor. Fiz. **65**, 2185 (1973) [Sov. Phys. JETP **38**, 1091 (1974)].
[68] A. S. Oganisyan, G. D. Petrov, and E. F. Yurchuk, Zh. Prikl. Spektrosk. **25**, 1111 (1976).
[69] O. V. Karpov, A. S. Oganisyan, G. D. Petrov, and E. F. Yurchuk, Zh. Prikl. Spektrosk. **29**, 415 (1978).
[70] V. M. Zolotorev, V. N. Morozov, and E. V. Smirnova, *Optical Constants of Natural and Optical Media* [in Russian], Khimiya, Leningrad, 1984.
[71] L. D. Landau and E. M. Lifshitz, *Electrodynamics of Continuous Media*, Pergamon Press, New York, 1983.
[72] A. E. Negin, V. P. Osipov, and A. V. Pakhomov, Kvant. Elektron. **13**, 2208 (1986) [Sov. J. Quantum Electron. **16**, 1458 (1986)].
[73] Yu. P. Raizer, Laser-Induced Discharge Phenomena, Consultants Bureau, N.Y., 1977.
[74] V. L. Ginzburg and A. V. Gurevich, Usp. Fiz. Nauk **70**, 201 (1960) [Sov. Phys. Usp. **3**, 115 (1960)].
[75] L. M. Biberman, V. S. Vorob'ev, and I. T. Yakubov, *Kinetics of Nonequilibrium Low-Temperature Plasma* [in Russian], Nauka, Moscow, 1982.
[76] A. V. Bondarenko, V. S. Golubev, E. V. Dan'shchikov, F. V. Lebedev, A. F. Nastoyashchii and A. V. Ryazanov, Pis'ma Zh. Tekh. Fiz. **5**, 221 (1979) [Sov. Tech. Phys. Lett. **5**, 87 (1979)].
[77] A. V. Bondarenko, V. S. Golubev, E. V. Dan'shchikov, F. V. Lebedev, A. F. Nastoyashchii, and A. V. Ryazanov, Dokl. Akad. Nauk SSSR **253**, 867 (1980) [Sov. Phys. Dokl. **25**, 616 (1980)].
[78] A. V. Bondarenko, E. V. Dan'shchikov, F. V. Lebedev *et al.* Kvant. Electron. **8**, 204 (1981) [Sov. J. Quantum Electron. **11**, 121 (1981)].
[79] A. V. Bondarenko *et al.*, Pis'ma Zh. Tekh. Fiz. **5**, 221 (1979) [Sov. Tech. Phys. Lett. **5**, 87 (1979)].
[80] E. V. Dan'shchikov, V. A. Dymshakov, F. V. Lebedev, and A. V. Ryazanov, Kvant. Elektron. **9**, 99 (1982) [Sov. J. Quantum Electron. **12**, 62 (1982)].
[81] E. V. Dan'shchikov, V. A. Dymshakov, F. V. Lebedev, and A. V. Ryazanov, Kvant. Elektron. **9**, 106 (1982) [Sov. J. Quantum Electron. **12**, 67 (1982)].
[82] E. V. Dan'shchikov, F. V. Lebedev, and A. V. Ryazanov, Fiz. Plazmy **10**, 385 (1984) [Sov. J. Plasma Phys. **10**, 225 (1984)].
[83] E. V. Dan'shchikov, V. A. Dymshakov, F. V. Lebedev, and A. V. Ryazanov, Kvant. Elektron. **12**, 1863 (1985) [Sov. J. Quantum Electron. **15**, 1231 (1985)].
[84] E. V. Dan'shchikov, V. A. Dymshakov, F. V. Lebedev, V. D. Pis'mennyi, and A. V. Ryazanov, Izv. Akad. Nauk SSSR, Ser. Fiz. **49**, 811 (1985).
[85] N. N. Rykalin and A. A. Uglov, Kvant. Elektron. **8**, 1193 (1985) [Sov. J. Quantum Electron. **11**, 715 (1981)].
[86] V. N. Smirnov, Zh. Tekh. Fiz. **48**, 1977 (1978) [Sov. Phys. Tech. Phys. **23**, 1127 (1978)].
[87] A. S. Kovalev and A. M. Popov, Zh. Tekh. Fiz. **50**, 333 (1980) [Sov. Phys. Tech. Phys. **25**, 196 (1980)].
[88] A. F. Nastoyashchii, Kvant. Elektron. **7**, 170 (1980) [Sov. J. Quantum Electron. **10**, 95 (1980)].
[89] A. A. Vedenov, G. G. Gladush, and A. N. Yavokhin, Kvant. Elektron. **8**, 1485 (1981) [Sov. J. Quantum Electron. **11**, 896 (1981)].
[90] A. A. Vedenov, G. G. Gladush, and A. N. Yavokhin, Fiz. Plazmy **9**, 434 (1983) [Sov. J. Plasma Phys. **9**, 255 (1983)].
[91] V. S. Vorob'ev and A. L. Khomkin, Pis'ma Zh. Tekh. Fiz. **9**, 1157 (1983) [Sov. Tech. Phys. Lett. **9**, 496 (1983)].
[92] V. S. Vorob'ev and A. L. Khomkin, Pis'ma Zh. Tekh. Fiz. **10**, 953 (1984) [Sov. Tech. Phys. Lett. **10**, 399 (1984)].
[93] V. S. Vorob'ev and A. L. Khomkin, Fiz. Plazmy **10**, 1025 (1984) [Sov. J. Plasma Phys. **10**, 589 (1984)].
[94] V. S. Vorob'ev and A. L. Khomkin, Kvant. Elektron. **11**, 2221 (1984) [Sov. J. Quantum Electron. **14**, 1478 (1984)].
[95] I. Yu. Borets-Pervak, V. S. Borob'ev, and S. V. Maksimenko, Pis'ma Zh. Tekh. Fiz. **16**, 68 (1990).
[96] V. S. Vorob'ev, S. V. Maksimenko, and A. L. Khimkin, Fiz. Plazmy **12**, 714 (1986) [Sov. J. Plasma Phys. **12**, 409 (1986)].
[97] V. S. Vorob'ev and S. V. Maksimenko, Kvant. Elektron. **14**, 1047 (1987) [Sov. J. Quantum Electron. **17**, 664 (1987)].
[98] A. L. Khomkin and B. P. Shelyukhaev, Teplofiz. Vys. Temp. **26**, 1066 (1988).
[99] F. L. Khomkin and B. P. Shelyukhaev, Contributed Papers, XX ICPIG, Pisa, 1989, p. 1023.
[100] I. Yu. Borets-Pervak and V. S. Vorob'ev, Kvant. Elektron. **18**, 999 (1991) [Sov. J. Quantum Electron. **21**, 905 (1991).
[101] C. J. Smithells, *Handbook of Metals* [Russian translation], Metallurgiya, Moscow, 1980.
[102] I. K. Kikoin [Ed.], *Handbook of Tables of Physical Quantities* [in Russian], Atomizdat, Moscow, 1976.
[103] D. A. Frank-Kamenetskii, *Diffusion and Heat Transfer in Chemical Kinetics* [in Russian], Nauka, Moscow, 1967.
[104] Yu. M. Sorokin, I. Ya. Korolev, and E. M. Krikunova, Kvant. Elektron. **13**, 2464 (1986) [Sov. J. Quantum Electron. **16**, 628 (1986)].
[105] S. V. Zakharchenko, S. N. Kolomiets, and A. M. Skripkin, Pis'ma Zh. Tekh. Fiz. **3**, 1339 (1977) [Sov. Tech. Phys. Lett. **3**, 552 (1977)].
[106] S. V. Zakharchenko, L. P. Semenov, and A. M. Skripkin, Kvant. Elektron. **11**, 2487 (1984) [Sov. J. Quantum Electron. **14**, 1642 (1984)].
[107] Yu. N. Zakharov, T. P. Kosoburd, and Yu. M. Sorokin, Zh. Tekh. Fiz. **54**, 969 (1984) [Sov. Phys. Tech. Phys. **29**, 579 (1984)].
[108] T. P. Kosoburd and Yu. M. Sorokin, Zh. Tekh. Fiz. **58**, 1318 (1988) [Sov. Phys. Tech. Phys. **33**, 785 (1988)].
[109] I. Ya. Korolev, T. P. Kosoburd, E. M. Krikunova, and Yu. M. Sorokin, Zh. Tekh. Fiz. **53**, 1547 (1983) [Sov. Phys. Tech. Phys. **28**, 952 (1983)].
[110] D. I. Zhukovitskii and I. T. Yakubov, Kvant. Elektron. **17**, 1084 (1990) [Sov. J. Quantum Electron. **20**, 999 (1990)].
[111] V. I. Bergel'son, A. P. Golub', I. V. Nemchinov *et al.*, Kvant. Elektron. No. 4, 20 (1973) [Sov. J. Quantum Electron. **3**, 288 (1974)].
[112] A. P. Golub', I. V. Nemchinov, A. I. Petrukhin *et al.*, Zh. Tekh. Fiz. **51**, 316 (1981) [Sov. Phys. Tech. Phys. **26**, 191 (1981)].
[113] G. S. Romanov and Yu. A. Stankevich, Dokl. Akad. Nauk BSSR **21**, 503 (1977).
[114] G. S. Romanov and Yu. A. Stankevich, Fiz. Khim. Obr. Materialov **4**, 15 (1981).
[115] A. M. Bonch-Bruevich, V. I. Zinchenko, Ya. I. Imas *et al.*, Zh. Tekh. Fiz. **51**, 919 (1981) [Sov. Phys. Tech. Phys. **26**, 551 (1981)].
[116] Tomas, RTiK **13**, 29 (1975).
[117] P. E. Nielsen, J. Appl. Phys. **46**, 4501 (1975).
[118] Pirri, RTiK **15**, 793 (1977).
[119] V. I. Bergel'son, T. I. Loseva, and I. V. Nemchinov, Prikl. Mekh. Tekh. Fiz. **4**, 22 (1974).
[120] I. V. Nemchinov, Izv. Akad. Nauk SSSR **746**, 1026 (1982).
[121] V. S. Golubev, L. I. Kiselevskii, and V. N. Snopko, Zh. Prikl. Spektrosk. **26**, 983 (1977).
[122] B. Steverding, J. Appl. Phys. **45**, 3507 (1974).
[123] V. S. Vorob'ev and S. V. Maksimenko, Teplofiz. Vys. Temp. **26**, 667 (1988).

[124] V. S. Vorob'ev, Teplofiz. Vys. Temp. **24**, 609 (1986).
[125] K. Sutton and T. M. Moss, AIAA Paper No. 79-0033, 1979.
[126] V. S. Vorob'ev and S. V. Maksimenko, Teplofiz. Vys. Temp. **26**, 852 (1988).
[127] M. V. Allmen, P. Blaer, K. Affolter, and E. Sturmer, IEEE J. **QE-14**, 85 (1978).
[128] I. Yu. Borets-Pervak and V. S. Vorob'ev, Kvant. Elektron. **18**, 1331 (1991) [Sov. J. Quantum Electron. **21**, 1216 (1991)].
[129] V. A. Danilychev, V. D. Zvorykin *et al.*, Kvant. Elektron. **7**, 2599 (1980) [Sov. J. Quantum Electron. **10**, 1518 (1980)].
[130] N. A. Babaeva, S. K. Belousov *et al.*, Kvant. Elektron. **13**, 493 (1986) [Sov. J. Quantum Electron. **16**, 323 (1986)].
[131] J. Herman, C. Boulmer-Leborgne, and B. Dubreuil, Appl. Surface Sci. **46**, 315 (1990)].
[132] J. Herman, C. Boulmer-Leborgne, I. N. Mihailescu, and B. Dubreil, J. de Phys. IV Colloque C7: Suppl au J de Phys. III 1, C7-709.
[133] J. Herman, C. Boulmer-Leborgne, B. Dubreil, and I. N. Mihailescu, J. Appl. Phys. **71**, 5629 (1992).
[134] K. Kagama S. Yokai, and S. Nakajima, Opt. Commun. **45**, 261 (1983).
[135] I. Yu. Borets-Pervak and V. S. Vorob'ev, Kvant. Elektron. **17**, 1044 (1990) [Sov. J. Quantum Electron. **20**, 959 (1990)].
[136] B. A. Raikhman and V. N. Smirnov, Zh. Tekh. Fiz. **47**, 1988 (1977) [Sov. Phys. Tech. Phys. **22**, 1155 (1977)].
[137] S. G. Burdin, I. N. Goncharov, V. I. Konov *et al.*, Izv. Akad. Nauk SSSR **46**, 1943 (1982).
[138] G. H. Canavan and P. E. Nielsen, Appl. Phys. Lett. **22**, 409 (1973).
[139] J. E. Lowder and H. J. Kleiman, J. Appl. Phys. **44**, 5504 (1973).
[140] N. N. Belov, Zh. Prikl. Matem. Teor. Fiz. **175**, 27 (1989).
[141] V. A. Volkov, F. V. Grigor'ev, V. V. Kalinovskii *et al.*, Zh. Eksp. Teor. Fiz. **69**, 115 (1975) [Sov. Phys. JETP **42**, 58 (1975)].
[142] N. N. Belov, N. P. Dashkevich, E. K. Karlova *et al.*, Zh. Tekh. Fiz. **49**, 333 (1979) [Sov. Phys. Tech. Phys. **24**, 193 (1979)].
[143] A. A. Bakeev, L. V. Vasil'ev, L. I. Nikolashina *et al.*, Zh. Prikl. Spektrosk. **3**, 592 (1979).
[144] A. A. Bakeev, B. A. Barikhin, B. B. Boronkov, *et al.*, Kvant. Elektron. **7**, 349 (1980) [Sov. J. Quantum Electron. **10**, 199 (1980)].
[145] Covington, Liu, and Lincoln, RTiK **15**, 148 (1977).
[146] L. Ya. Min'ko, *Preparation and Investigation of Pulsed Plasma Flows* [in Russian], Nauka, i tekhnika, Minsk, 1970.
[147] A. P. Golub', T. V. Loseva, and I. V. Nemchinov, Fiz. Khim. Obrat. Materialov, No. 1, 27 (1981).
[148] S. A. Metz, L. R. Hattoche, R. L. Stegman *et al.*, J. Appl. Phys. **46**, 1634 (1975).
[149] V. A. Batanov, F. V. Bunkin, A. M. Prokhorov *et al.*, Pis'ma Zh. Eksp. Teor. Fiz. **11**, 113 (1970) [JETP Lett. **11**, 69 (1970)].
[150] A. V. Burmistrov, Zh. Tekh. Fiz. **48**, 2313 (1978) [Sov. Phys. Tech. Phys. **23**, 1325 (1978)].
[151] V. N. Smirnov, Zh. Tekh. Fiz. **48**, 1977 (1978) [Sov. Phys. Tech. Phys. **23**, 1127 (1978)].
[152] V. N. Smirnov and Vl. N. Smirnov, Zh. Tekh. Fiz. **48**, 860 (1978) [Sov. Phys. Tech. Phys. **23**, 504 (1978)].
[153] A. M. Avilov, V. D. Volovik, A. A. Evtukh *et al.*, Zh. Tekh. Fiz. **52**, 2071 (1982) [Sov. Phys. Tech. Phys. **27**, 1271 (1982)].
[154] M. I. Molotskii, Fiz. Tverd. Tela **19**, 642 (1977) [Sov. Phys. Solid State **19**, 374 (1977)].
[155] I. Volbrant, Yu. A. Khrustalev, E. Linke *et al.*, Dokl. Akad. Nauk SSSR **225**, 342 (1975).

Translated by M. E. Alferieff